Synthesis and Characterization of Dimethylbismuth and -Indium Phenoxy-imine Complexes as Potential Catalysts for the Ring Opening Polymerization of Cyclic Esters

By

Kathleen Morrison

A thesis submitted to the
Department of Chemistry and Biochemistry
Mount Allison University
in partial fulfillment of the requirements for the
Bachelor of Science degree with Honours

April 2019

Thesis Committee

Supervisor

Dr. Glen Briand
Associate Professor of Chemistry

Reviewer

Dr. Stephen Westcott
Professor of Chemistry

Table of Contents

Acknowledgments

I would like to acknowledge the people who have been instrumental to the success of my Honours project and thesis. First and foremost, thank you to my Honours supervisor, Dr. Glen Briand, who has endlessly supported me, on top of any and every student who seeks his help. His encouragement, enthusiasm and advice has enabled my growth as a student, my passion for crystals and has inspired me to pursue a Master's in Chemistry.

Thank you to Dr. Steve Westcott for being my second reader and who initially fostered my interest in inorganic chemistry in my second year at Mount Allison. I would also like to thank Dan Durant for his NMR expertise and assistance and Phil Cormier for the training he has provided. I would like to thank Dr. Jason Masuda at Saint Mary's University for the X-ray crystallography analysis. Thank you to the Natural Science and Engineering Research Council of Canada for their funding of my summer research that has made this project possible. I would like to acknowledge the Department of Chemistry and Biochemistry at Mount Allison for the opportunity to conduct research and the support that has been provided for me and many other students.

To Marcus Kindervater, Adam Beckett and Sarah Martell, you three are one of the reasons I love research. The connections I have made are lifelong and rooted in memories of Big Dog, our dancing and singing in the lab, Marcus destroying us in basketball, group meetings on the back deck, and Sara and Vlad making me laugh excessively. Thank you to Gus Doane, Lauren Wentzell and Rachel Vanderkloet for the support, laughs and friendship.

Finally, thank you to my friends, family, basketball teammates and coffee who have an undying willingness to help me achieve, cheer me on, help carry my load and remind me to not take myself too seriously.

List of Figures

List of Schemes

List of Spectra in Appendix

Glossary of Abbreviations and Symbols

Ar	Aryl
cm^{-1}	Wavenumber
d	Doublet
D	Deuterium
Et	Ethyl
Equiv.	Equivalents
g	Gram
h	Hour
Hz	Hertz
IR	Infrared
J	Coupling constant
L	Ligand
m	Multiplet or medium
M	Molarity (mol L^{-1})
Me	Methyl
min	Minutes
mL	Milliliter
mmol	Millimole
mol	Mole
mp	Melting point
MW	Molecular weight
NMR	Nuclear Magnetic Resonance

PLA	Poly(lactic acid)
rac	Racemic
ROP	Ring opening polymerization
s	Singlet or strong
tBu	*tert*-butyl
THF	Tetrahydrofuran
vw	Very weak
w	Weak
°	Degree
°C	Degrees Celsius
Å	Angstrom
δ	Chemical shift
^{1}H	Hydrogen-1 nuclei
$\{^{1}H\}$	Proton-decoupled
^{13}C	Carbon-13 nuclei

Abstract

Traditional plastics and polymers, that began to be mass produced in the 1940's, are petrochemically derived and lack renewability, biodegradability and sustainability. Further, their use and production does not satisfy the principles of "Green Chemistry". The consequences surrounding the use of plastics can be avoided through the development of biodegradable plastics, or bioplastics. The most extensively studied and industrially available bioplastic is poly(lactic acid), which can be synthesized through the ring opening polymerization (ROP) of cyclic esters. This reaction requires a catalyst, where metal alkoxide species have been found to been effective. However, there are issues of toxicity and high cost related to the species currently being used, which poses an opportunity for new catalyst development. A more environmentally friendly option is using bismuth and indium as metal centres in these catalysts as they are both relatively non-toxic, inexpensive and reactive. Therefore, this research focuses on the synthesis and characterization of novel dimethylbismuth and -indium phenoxy-imine complexes for the ROP of cyclic esters. It was determined that the three target phenoxy-imine supported bismuth complexes can be generated *in situ*, however, their hydrolytic instability disallows recrystallization of these complexes. Contrastingly, the three target phenoxy-imine indium complexes were all successfully synthesized and characterized by ^{1}H NMR, $^{13}C\{^{1}H\}$ NMR, FT-IR and FT-Raman spectroscopy. Indium complexes **5** and **6** have been analyzed by X-ray crystallography.

1. Introduction

1.1 Principles of Green Chemistry

The field of green chemistry is becoming increasingly important and is continually growing. It has value from an environmental standpoint, it is proving to be economically favourable, and is finding improvements in safety. Green chemistry was initially developed in the early 1990's and has since created a cascade of initiatives that have made the principles of green chemistry prominent in industrial and academic settings.[1] These goals include the design of safer chemicals, prevention of waste and the use of less hazardous materials. Moreover, green chemistry is driven by its focus on precise design of chemical processes to improve safety and renewability, as well as decrease impact on the environment. The principles or defining features of green chemistry can result in economic profitability due to improved cost, energy and time efficiency.[1]

The twelve principles of green chemistry were developed by John Warner and Paul Anastas in 1998 to help provide a framework for chemists to employ green processes as well as improve safety and sustainability in their work (Figure 1).[1] The principles of green chemistry are a major focus of this work. Of the twelve principles, four are considered most pertinent to this study: use of catalysts; use of renewable feedstock; less hazardous substances; and design of safer chemicals. The first promotes the use of catalytic reagents instead of stoichiometric reagents due to the ability of catalysts to lower the activation energy and improve the efficiency of a reaction. The second promotes the use of renewable feedstock to improve the sustainability of a process. The third and fourth state that the design of chemical procedures should be made to use and produce substances that are minimally toxic for the betterment of human and environmental safety. Encompassing as many as these principles into

chemical procedures and processes will yield improvement in sustainability, safety, renewability and potential for a method with economic profitability that could be implemented in an industrial setting.[2]

Figure 1. Twelve principles of green chemistry.

The principles of green chemistry have been applied to the plastics industry where, traditionally, plastics were petrochemically derived and non-sustainable. More recently, renewable, biodegradable, and biocompatible polymers have been studied and found to be viable replacements for traditionally derived plastics. Finding a more environmentally friendly alternative for traditional plastics is the foundation of this study and highlights the importance of green chemistry in everyday applications.

1.2 Petrochemically Derived Plastics

In the 1940's, plastics were mass produced and were soon considered a necessary material in everyday life, industry and medicine. Its rapid rise to success as a material is based upon its cost- and energy-efficiency and the versatility of its properties. The long chain compounds that are characteristic of plastics, such as polyethylene and polypropylene (Figure 2), are comprised of monomer units that were traditionally petrochemically derived.[3] Materials produced from petrochemicals lack renewability, sustainability, biocompatibility and biodegradability and therefore do not fulfil the twelve principles of green chemistry. The copious amounts of petrochemically derived disposed plastics have exposed humans to toxic chemicals including di-(2-ethylhexyl) phthalate (DEHP) and bisphenol-A (BPA), shown in Figure 3.[3]

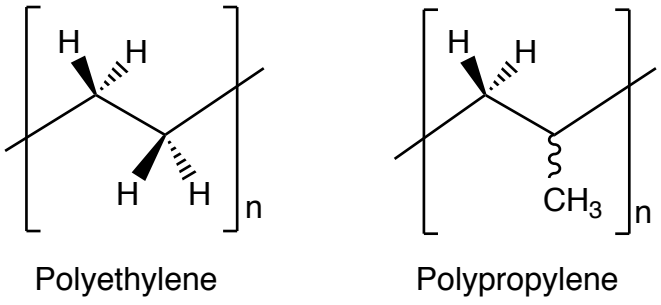

Figure 2. Petrochemically derived plastics.

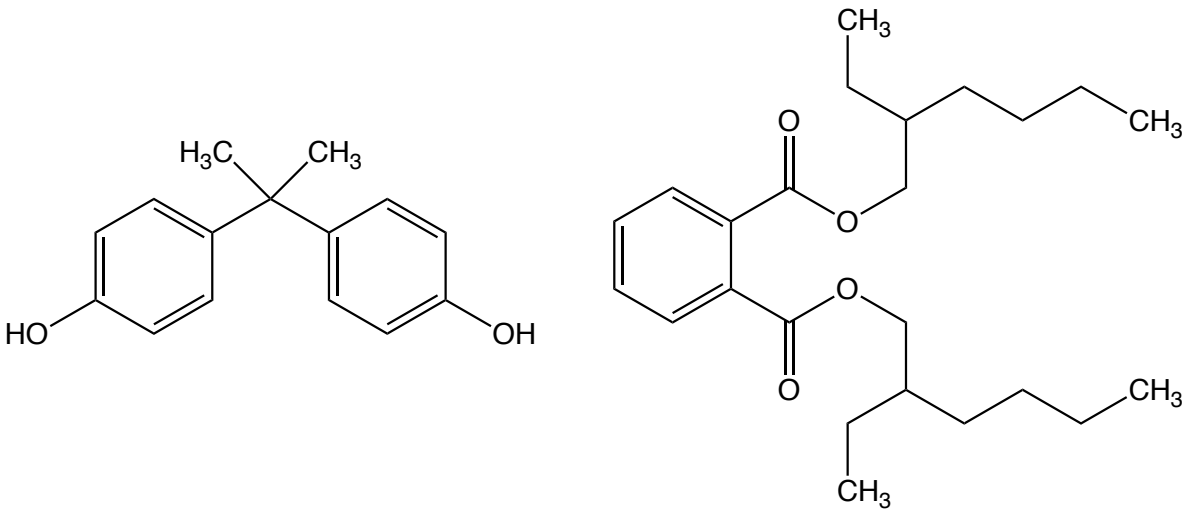

BPA DEHP

Figure 3. Toxic chemicals in petrochemically derived plastics, bisphenol-A (BPA) and di-(2-ethylhexyl) phthalate (DEHP).

Disposal of plastics is an important issue due to the material often having one-time use. The common ways plastic is disposed of include: landfilling, incineration, recycling and biodegradation. Recycling is a viable means of dealing with used plastics as it recovers the plastic material without directly contributing to greenhouse gas emissions.[3] However, recycling relies on people to sort their waste properly, which has proven to be a challenge and in turn most plastic ends up in landfills. The notion of landfilling is not entirely negative as it does not directly contribute to greenhouse gas emissions. However, it does require land availability that is limited, contributes to long-term pollution and is not sustainable. Incinerating plastics can be an effective method of disposal, but measures must be taken to ensure that the quality and composition of air is not effected. Incineration tends to release greenhouse gases including carbon dioxide, dioxins and polycyclic aromatic hydrocarbons.[3] Finally, biodegradation is the best option when the process is designed appropriately. Using the guiding principles of green chemistry, polymers can be designed to be biodegradable and

thus degrade into products that are not harmful to the environment. Biodegradation involving polymers that are not petrochemically derived circumvents greenhouse gas emissions and long-term pollution.[4]

1.3 Biodegradable Plastics

The increased production and interest in bio-based materials has coincided with growth in the use of green chemistry. Biodegradable polymers serve as an environmentally friendly alternative to traditional plastics that are petroleum-based as they are able to naturally decompose in the environment. The enzymatic action of microorganisms and chemical hydrolysis break down biodegradable polymers into smaller units.[5] An important requirement for degradation of these polymers is that the hydrolysis reactions occur over the course of two months at temperatures of up to 50°C and result in products that are non-toxic. Natural products that result from polymer degradation and cause no harm to the environment include carbon dioxide, methane, water, humic matter and biomass.[5]

There are various types of biodegradable polymers including polyesters, polyurethanes and polyanhydrides. These synthetic products can be achieved by choosing reactants that give the desired properties for the final product. Due to the biocompatibility and versatile properties of polyesters, they are a more heavily investigated polymer for application as alternatives to traditional plastics.[6] Poly(α-esters) contain a reactive aliphatic ester linkage and are considered strong thermostatic polymers that fall under the general class of aliphatic esters. Additionally, poly(α-esters) is a class of polyesters containing poly(α-hydroxy acids) such as poly(glycolic acid), polylactides, poly(lactic acid) (PLA), and other copolymers.[6] Polylactides are prepared by ring opening polymerization (ROP) of lactide and their general structure is shown in Figure 4. The degradation of polylactides is easily facilitated through hydrolysis of the ester bond,

which produces the nontoxic product lactic acid. The fermentation of polysaccharides in corn and potatoes enables lactic acid to be obtained with ease and in a cost-efficient manner.[7] Polymerization of lactic acid can then be achieved through a condensation reaction, or it may be dimerized into a lactide ring and later polymerized through ROP. Dissimilar to petrochemically derived plastics, the incineration of polylactides plastics does not result in harmful products. Therefore, PLA is an interesting green plastic that is used for various applications in industry. Moreover, biodegradable polymers find purpose in tissue engineering, coatings on implants, packaging materials and gene therapy.[6]

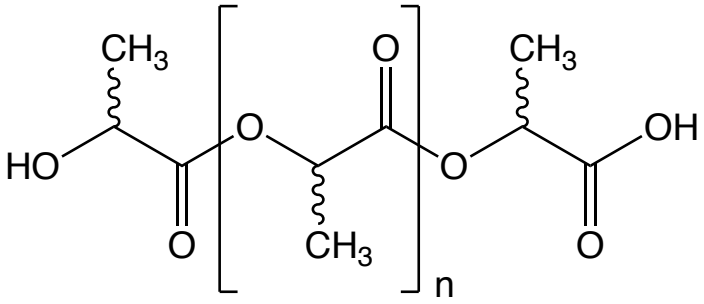

Figure 4. General structure of polylactide.

1.4 Synthesis of Biodegradable Plastics

The polymerization reactions that are used to produce biodegradable polymers employ monomer units that are high in purity. The presence of water, for example, is considered an impurity that can disrupt these polymerization reactions. Hydroxyl and carboxylic functional groups are also considered impurities that can have an effect on polymerization. Direct polycondensation, azeotropic condensation, solid-state and ROP are the main methods used to synthesize biodegradable plastics.[7] For this study, the synthesis method of focus is ROP, where lactide, a cyclic dimer of lactic acid, is required. As lactic acid has two stereoisomers, three forms of lactide can be produced (Figure 5). ROP is a beneficial method as it allows for the

physical properties and stereo-regulation of the polymer to be controlled. There are different reaction mechanisms observed the for the ROP process, including cationic, anionic and coordination-insertion.[8] The mechanism of interest for this study is coordination-insertion.

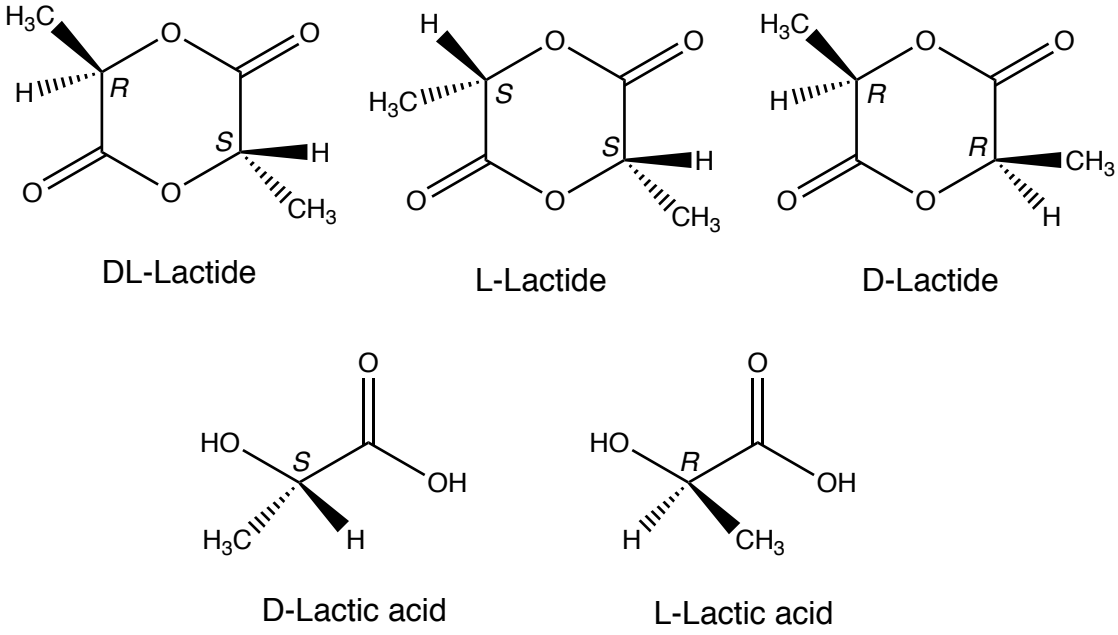

Figure 5. Lactic acid and lactide monomer isomers.

1.5 Ring Opening Polymerization (ROP) of Cyclic Esters

Ring opening polymerization (ROP) is the favoured method for polymerization of cyclic esters. The ROP of lactide in the production of PLA yields higher molecular weights (MWs), stereocontrol over the resulting polymer and lower polydispersites.[7] Using ROP, the most efficient synthetic method for producing PLA is through the use of a metal catalyst that follows the coordination-insertion mechanism (Scheme 1). The catalyst that is used tends to be a metal alkoxide species as they behave as weak Lewis acids and contain empty p or d orbitals at a

desirable energy level. The propagating species tends to be formed *in situ* from a metal-alkyl and an alcohol initiator, where the alcohol replaces an alkyl group on the metal centre.[9]

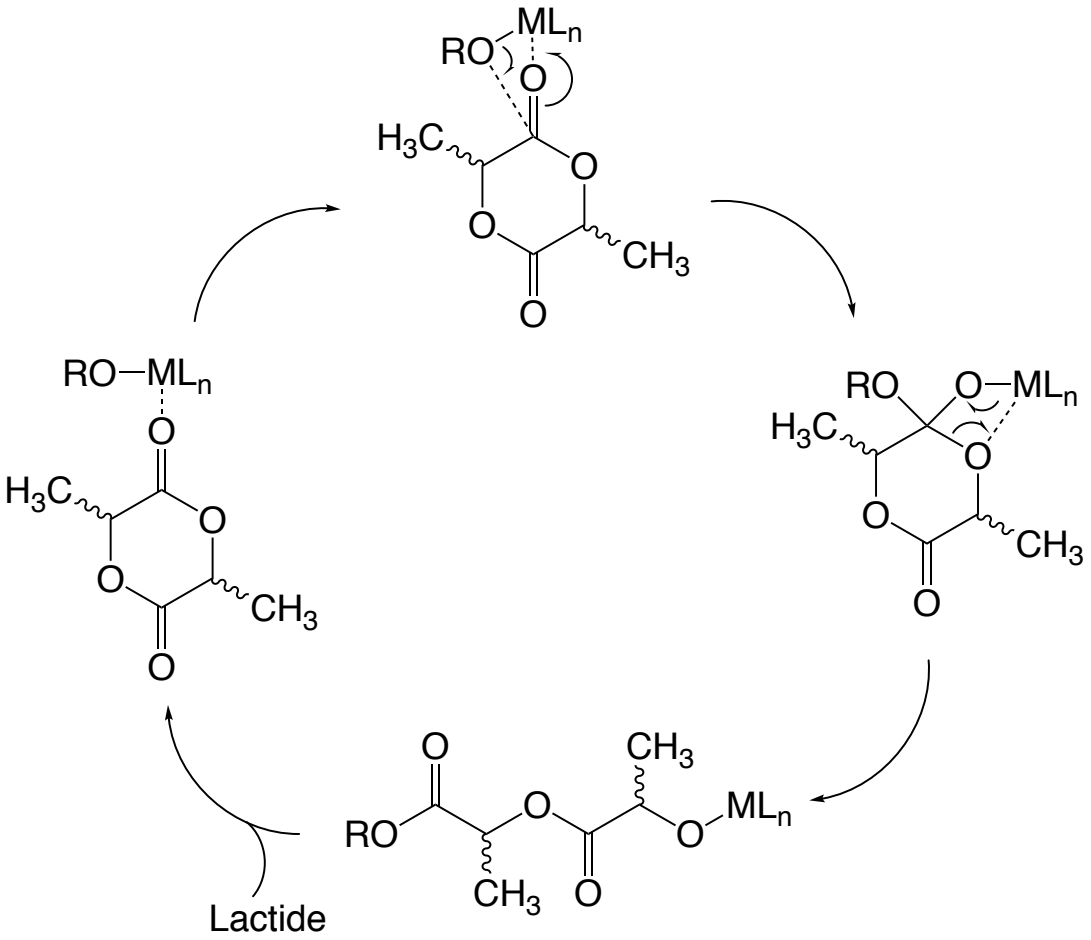

Scheme 1. Proposed coordination-insertion mechanism for a metal catalyzed ROP of cyclic esters.

Following the initiation step, the catalytic cycle commences with the cyclic ester coordinating to the catalyst through the carbonyl oxygen bound to its Lewis acidic metal centre. This coordination causes an increase in nucleophilicity of the catalyst's alkoxide region and concurrently increases the electrophilicity of the carbonyl on the lactide monomer.[7] These changes allow for the monomer to be inserted into the metal alkoxide bond through a

nucleophilic attack of the alkoxide on the carbonyl carbon. The cleavage of the acyl-oxygen bond opens the lactide ring and the configuration is retained. The polymerization is able to continue while the polymer chain continues to be coordinated to the metal centre of the catalyst. This metal alkoxide species subsequently adds additional monomer units.[10]

1.6 Polymers

There are a variety of applications that polymers have in numerous fields of study. The different traits of polymers include their MW, polydispersity and polymer tacticity. Polydispersity is the distribution of molecular mass in a specific polymer and polymer tacticity is the stereochemistry of adjacent stereocentres.[11] Through the use of either D- or L-lactic acid, lactide monomers can be achieved with differing diastereomer forms (D, L, DL; Figure 5). When D- and L-lactide are in a racemic mixture the diastereomers are denoted as *rac*-lactide and the name *meso*-lactide signifies that the DL-lactide has been used. Due to the variation in feedstocks from which lactide rings can be obtained, there are four lactide stereoisomers that result: D- or L-lactide, *rac*-lactide and *meso*-lactide.[12]

Due to the possibility of using the different diastereomeric forms in ROP, several polymer microstructures are obtained, which include: isotactic, heterotactic, syndiotactic and atactic (Figure 6).[12] Isotactic polymers are generated from pure lactide isomers where the same chirality is found at all chiral centres (*RRRR* or *SSSS*). The stereochemical configuration in syndiotactic polymers alter along with backbones of the polymer (*RSRS*), which is obtained by the ROP of *meso*-lactide. Heterotactic polymers, achieved using *meso*-lactide and *rac*-lactides, have alternating stereocentre units (*RRSS*). The backbone of atactic polymers have random stereochemical configurations.

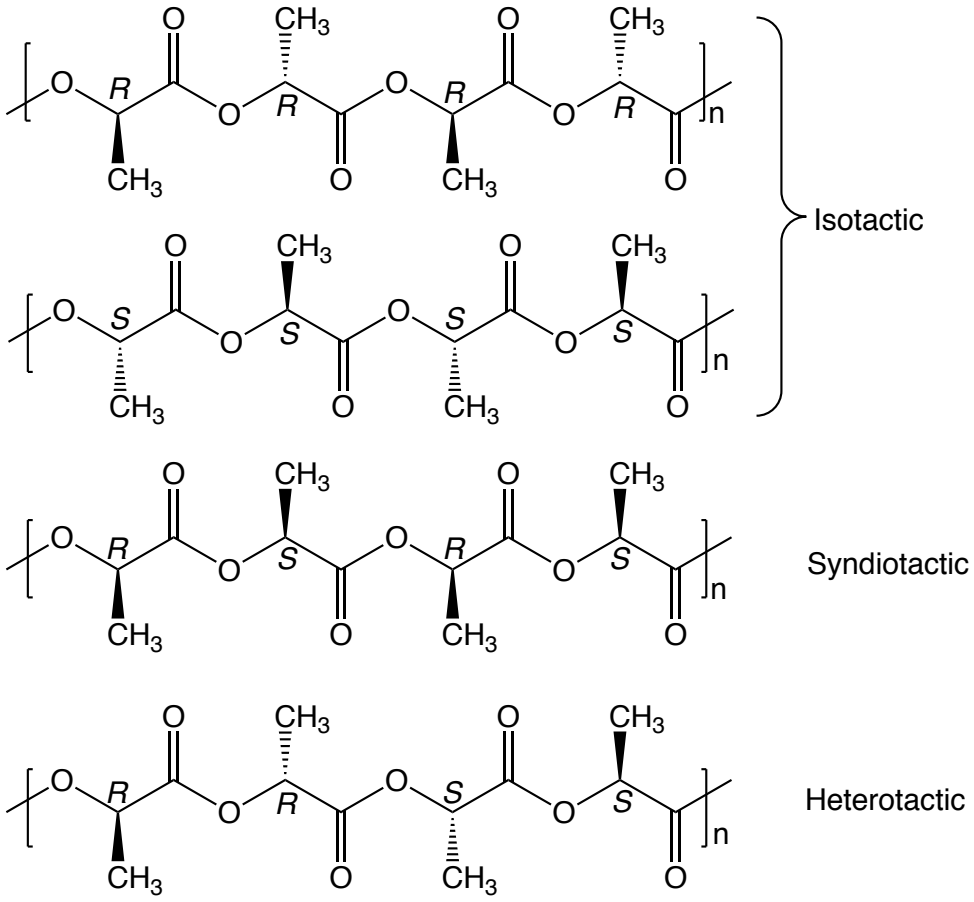

Figure 6. Polymer tacticities for polylactides.

1.7 Bismuth Catalysts

The most studied and traditionally most effective catalysts for the ROP of cyclic esters tend to possess metal centres (e.g. aluminum and tin). Aluminum iminophenolate complexes (Figure 7) have been extensively studied for the catalysis of ROP reactions and have been deemed some of the most effective. Tin(II) octanoate effectively and efficiently catalyzes the ROP of *rac*-lactide to afford atactic PLA.[14] However, aluminum and tin compounds are generally considered to be toxic and there is some evidence that the former is linked to

Alzheimer's disease.[13] Therefore, many of these effective catalysts have been deemed undesirable as trace amounts of the catalysts are found within the polymer.[14]

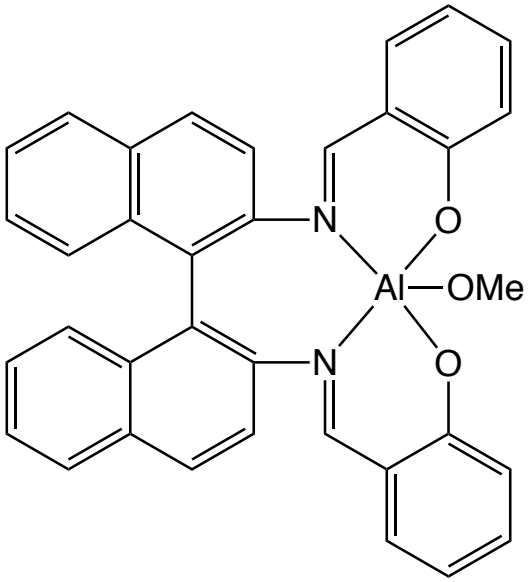

Figure 7. Structure of an aluminum alkoxide catalyst.

There has been increased interest in using alternative metal centres that are more environmentally benign and satisfy the principles of green chemistry. Bismuth-based catalysts have desirable properties for the catalysis of ROP reactions due to their relatively low toxicity, reactivity and cost efficiency.[15] Bismuth is a heavy p-block metal that exists in the 3+ and 5+ oxidation states and is located in group 15 on the periodic table. In spite of it being a heavy metal, it is both non-toxic and non-carcinogenic, which allows for its application in the field of medicinal chemistry. One of the main uses of bismuth in medicine is in the treatment of issues regarding the gastrointestinal tract. Bismuth subsalicylate is the active ingredient in Pepto-Bismol, which is used to treat common digestive problems in the human body. Another example of the use of bismuth in medicine is in bismuth subcitrate, which is a compound used to treat more serious digestive problems including peptic ulcers.[16] The properties of bismuth

make it suitable to be used in the development and study of products and procedures that are aimed to be more conducive to green chemistry.

In addition to treating digestive problems, bismuth subsalicylate has also been tested as a catalyst in the ROP of lactides. It was determined that bismuth subsalicylate is an active and effective catalyst for this reaction. The reaction mechanism for bismuth subsalicylate yields heterotactic PLA from *rac*-lactide.[17] The results for this bismuth compound were compared to that of the industrially used catalyst, tin(II) octanoate. Upon comparison, it was noted that the two compounds are assumed to follow a similar mechanism due to the M-OR initiator group present in both. However, bismuth subsalicylate was found to be slightly less reactive.[17]

Recently, it was determined that bis(imine)-bis-phenolate (salen) bismuth compounds proved to act as effective catalysts for ROP reactions.[8] Specifically, (Cy-salen)Bi(OtBu) and (Cy-salen)Bi(O-2,6-tBuC_6H_3) (Figure 8) were active catalysts for the ROP of L- and *rac*-lactide. In comparison to tin(II) octanoate, the reactivity of the bismuth catalysts was found to be higher at room temperature. However, these bismuth catalysts have been reported to be very unstable due to their moisture sensitivity.[8]

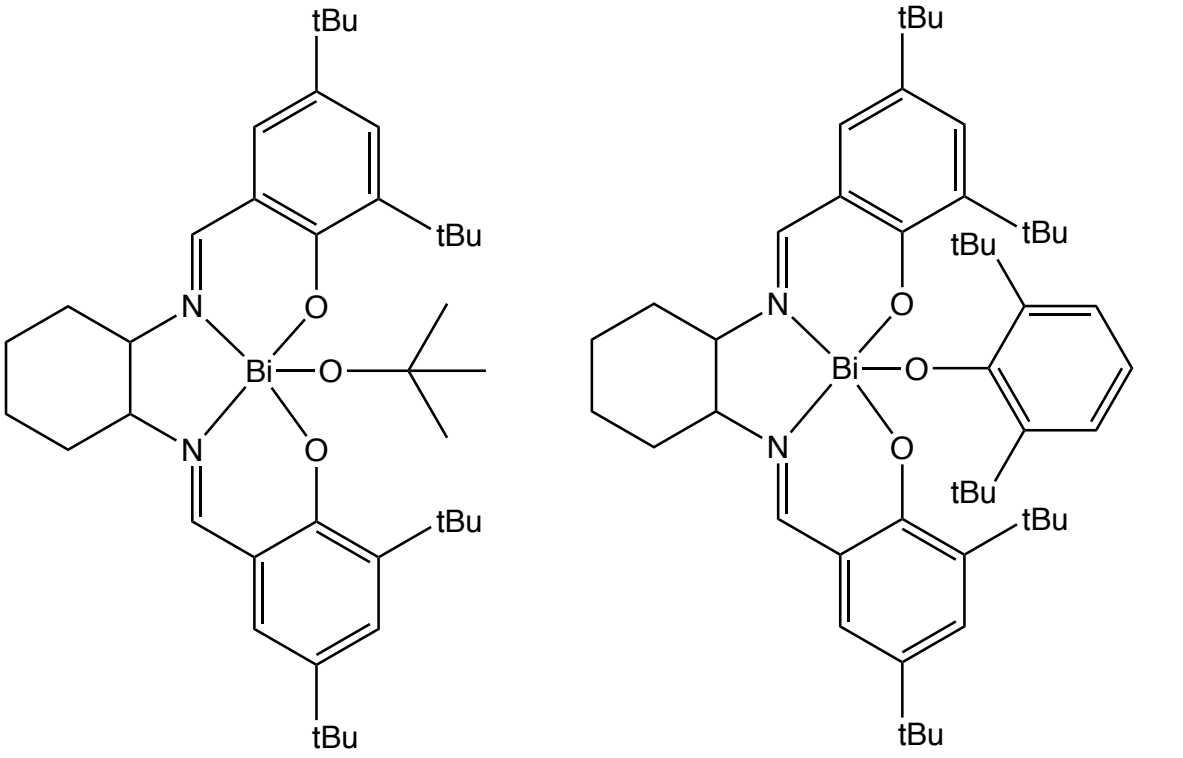

(cy-salen)BiOBu^t (cy-salen)BiOC$_6$H$_3$-2,6Bu$^t_2$.

Figure 8. Cy-salen supported bismuth complexes.

1.8 Indium Catalysts

Indium is a heavy p-block metal located in group 13 on the periodic table that is stable in both the +1 and +3 oxidation states, with the latter being more stable. Its most common use is in indium tin oxide, which is a component of cellphone screens, flatscreen televisions and solar panels.[18] Some indium-based compounds have been used as effective catalysts for the ROP of cyclic esters. Comparisons to other previously studied catalysts have shown that some of these species have potential as effective initiators as they are equal or more effective than the alternatives.[19]

Comparably to bismuth, indium is relatively non-toxic. Indium compounds tend to be stable in air and water and are often able to act as Lewis acids. It has been noted that indium catalysts have greater functional-group tolerance in a number of organic reactions in comparison to aluminum analogues.[19] One of the first indium catalysts reported for the ROP of lactides was an alkoxy-bridged dinuclear indium complex (Figure 9). It was found that this chiral compound is an active catalyst for the ROP of cyclic esters and that the conversion rate of *rac*-lactic acid to PLA is faster than with aluminum salen complexes. This finding has evoked increased interest and research into the use of indium-based catalysts for ROP reactions.[18]

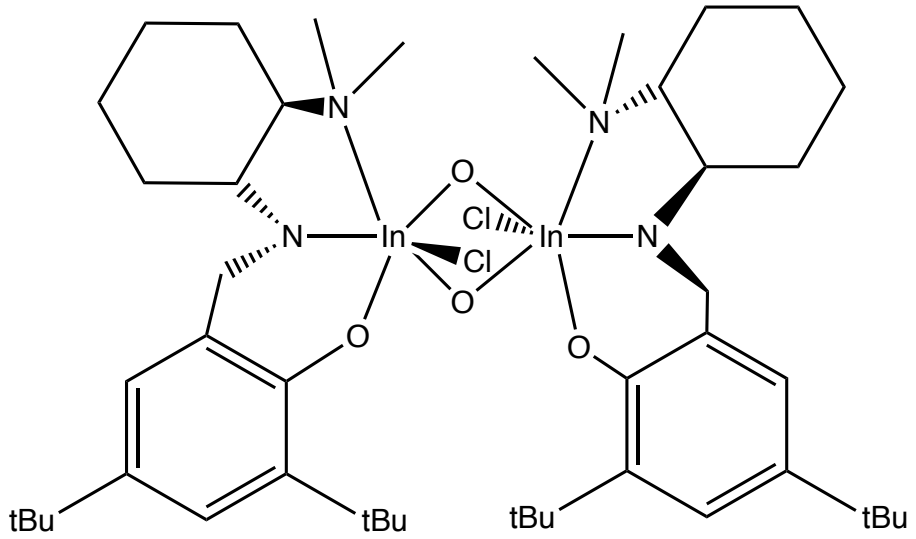

Figure 9. Active indium-based catalyst for the ROP of cyclic esters.

1.9 Phenoxy-imine Ligands

Ligand design can affect the reactivity, selectivity and overall activity of a catalyst. Schiff bases can be readily synthesized through a condensation reaction between a primary amine and an aldehyde. Phenoxy-imine ligands, synthesized through Schiff base condensation reactions, find applications in coordination chemistry, bioorganic chemistry and catalysis.[20]

Further, their metal complexes have been found to catalyze polymerization reactions, epoxidation reactions, Suzuki cross-coupling reactions, and many others. The tunability of the sterics and electronics of these ligands and their straight forward synthesis, both contribute to the interest and use of these ligands in chemistry.[20]

The use of phenoxy-imine metal complexes as catalysts for the ROP of cyclic esters has been studied. Several aluminum complexes containing a series of phenoxy-imine ligands (Figure 10) have proven to be effective catalysts for ROP of cyclic esters.[21] Other metal phenoxy-imine species that have been studied include nickel, copper and iron, to name a few.[20] However, the corresponding indium and bismuth complexes have not been reported.

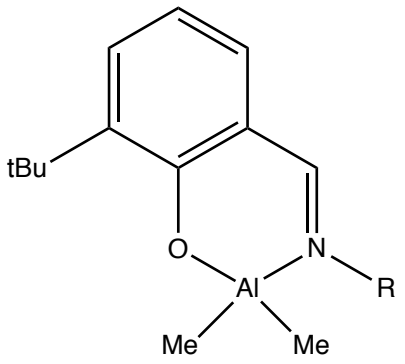

R = tBu, cyclohexyl, adamantyl, C_6H_5, 2,6-$Me_2C_6H_3$, 2,4,6-$Me_3C_6H_2$, 2,4,6-$tBu_3C_6H_2$, C_6F_5

Figure 10. Effective phenoxy-imine supported aluminum catalysts for ROP of cyclic esters.

1.10 Current Study

The current study aims to synthesize and characterize dimethylbismuth and -indium phenoxy-imine complexes and test them as potential catalysts for the ROP of cyclic esters. The use of bismuth and indium aims to improve the design of ROP catalysts while following the principles of green chemistry. The three ligands that will used in this study (Figure 11) are

synthesized through a condensation reaction between 3,5-di-tert-butyl-2-hydroxybenzaldehyde and a primary amine, namely tert-butylamine, cyclohexylamine or 2,4,6-trimethylaniline to produce **HL1**, **HL2** and **HL3**, respectively. These ligands have varying bulkiness, which allows for the reactivity of each catalyst to be tested and compared.

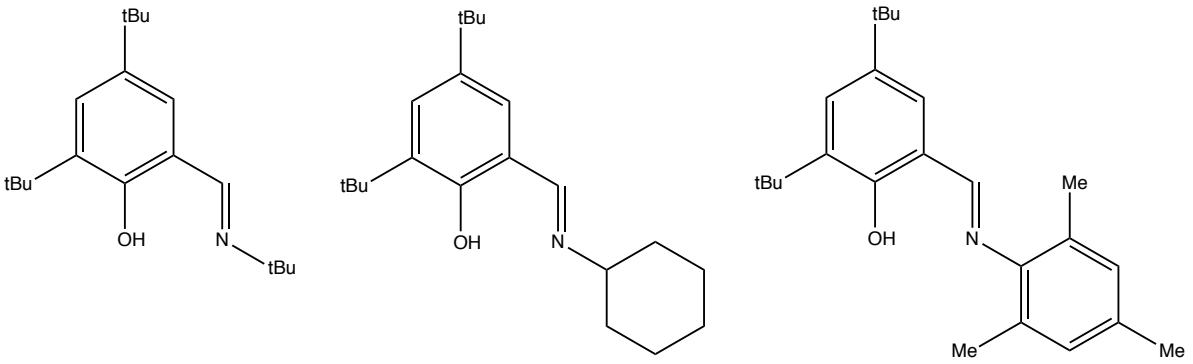

HL1, R = tBu **HL2**, R = cyclohexyl **HL3**, R = 2,4,6-$Me_3C_6H_2$

Figure 11. Phenoxy-imine ligands used in the synthesis of target indium and bismuth complexes.

The target bismuth complexes (Figure 12) will be achieved by a metathesis reaction between the deprotonated ligand and a dimethylbismuth halide. The target indium complexes (Figure 12) will be synthesized through a hydrocarbon elimination reaction of the imino-phenol and trimethylindium. The ligands and complexes will be characterized by ^{1}H NMR and $^{13}C\{^{1}H\}$ NMR spectroscopy, FT-IR spectroscopy, FT-Raman spectroscopy, and X-ray crystallography. Following the successful synthesis and characterization of the target complexes, they will be tested as catalysts for the ROP of cyclic esters for the production of aliphatic polyesters.

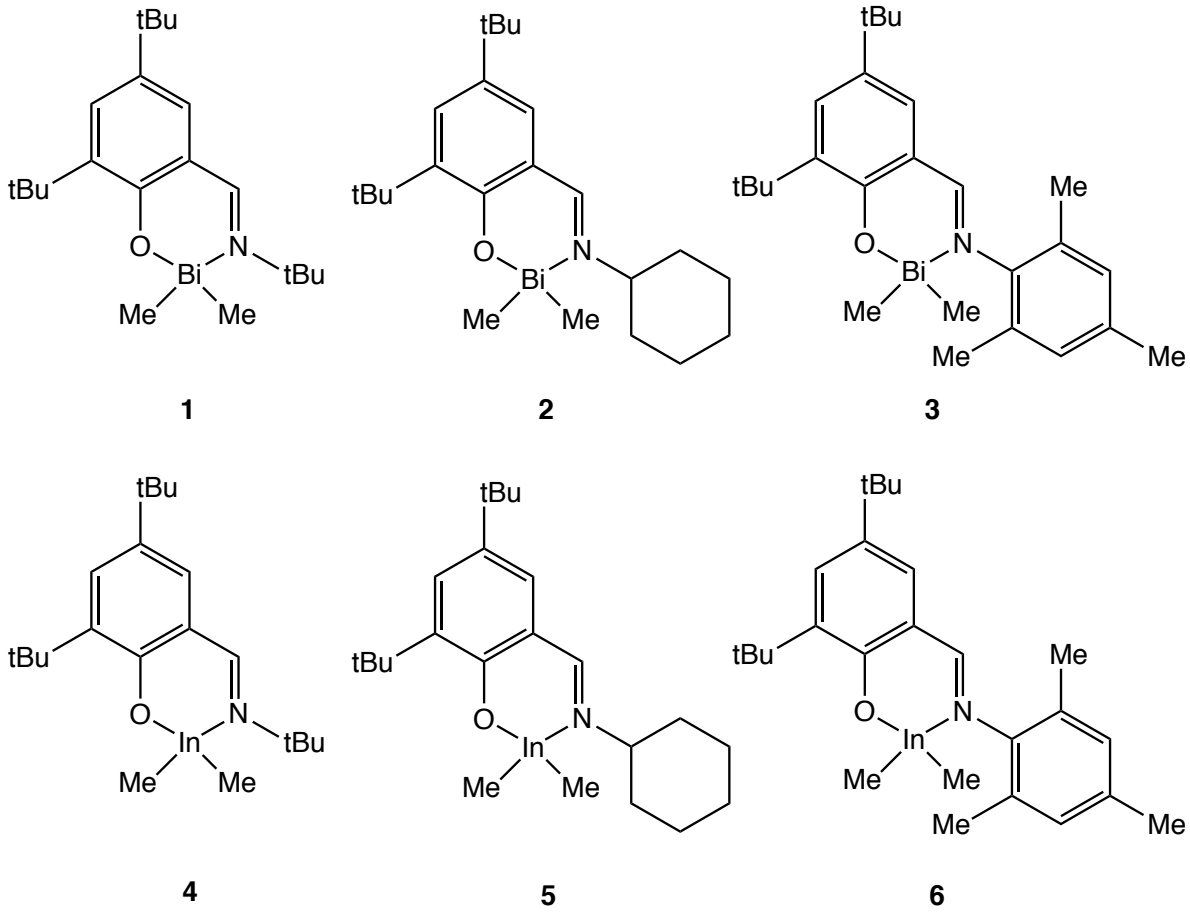

Figure 12. Target bismuth and indium complexes for this study.

2. Experimental

2.1 Instrumentation

An Innovative Technology glove box and Schlenk line techniques with a dinitrogen atmosphere, were used for the all air and moisture sensitive reactions. ^{1}H NMR and ^{13}C{^{1}H} NMR spectra were obtained using a Varian Mercury 200 MHz+ Spectrometer (^{1}H: 200 MHz) or a JEOL ECS-400 MHz Spectrometer (^{1}H: 400 MHz) at 23˚C. FT-Raman spectra were recorded on a Thermo Nicolet NXR 9650 FT-Raman Spectrophotometer. Melting points were recorded on an Electrothermal MEL-TEMP melting point apparatus. ATR FT-IR spectra were recorded on a Thermo Nicolet iS5 FT-IR spectrometer in the range of 4000-400 cm^{-1}.

2.2 Reagents

Tert-butylamine 98%, cyclohexylamine ≥99.9%, 2,4,6-trimethylaniline 98%, 3,5-di-*tert*-butyl-2-hydroxybenzaldehyde 99%, methyllithium solution 1.6 M in diethyl ether, bismuth(III) bromide anhydrous powder 99.999% trace metals basis, methanol and ethanol were used as received from Sigma Aldrich. Trimethylindium 98+% was used as received from Strem. Molecular sieves and sodium metal were added to dichloromethane, tetrahydrofuran (anhydrous, ≥99.9%, inhibitor-free), toluene anhydrous 99.8%, hexanes anhydrous 95% and diethyl ether anhydrous ≥99%, received from Sigma Aldrich. Phenoxy-imine ligands[22,23] and dimethylbismuth bromide[24] were synthesized using modified literature procedures.

2.3 Ligand Synthesis

2.3.1 Synthesis of HL1[22]

Tert-butylamine (1.56 g, 21.3 mmol) was added to a solution of 3,5-di-*tert*-butyl-2-hydroxybenzaldehyde (5.00 g, 21.3 mmol) in methanol (50 mL). This solution was left to stir for 24 h and the yellow precipitate was collected by suction filtration (4.87 g, 21.3 mmol, 79%). The crude product was recrystallized with wet and again in dry dichloromethane, which yielded a yellow crystalline product. ^{1}H NMR ($CDCl_3$, ppm): δ = 1.32 [s, 9H, $C(CH_3)_3$], 1.35 [s, 9H, $C(CH_3)_3$], 1.47 [s, 9H, $C(CH_3)_3$], 7.10 (d, $^{4}J_{HH}$ = 2.4 Hz, 1H, Ar-H), 7.37 (d, $^{4}J_{HH}$ = 2.6 Hz, 1H, Ar-H), 8.36 (s, 1H, N=CH), 14.59 (s, 1H, OH).

2.3.2 Synthesis of HL2[22]

Cyclohexylamine (2.12 g, 21.3 mmol) was added to a solution of 3,5-di-*tert*-butyl-2-hydroxybenzaldehyde (5.00 g, 21.3 mmol) in methanol (50 mL). The solution was left to stir for 24 h and the yellow precipitate was collected by suction filtration (6.03 g, 21.3 mmol, 89%). The crude product was recrystallized with wet and dry dichloromethane, yielding a

yellow crystalline product. ^{1}H NMR ($CDCl_3$, ppm): δ = 1.20–1.85 (m, 10H, cyclohexyl-H), 1.31 [s, 9H, $C(CH_3)_3$], 1.46 [s, 9H, $C(CH_3)_3$], 3.12 (m, 1H, cyclohexyl-H), 7.08 (d, $^{4}J_{HH}$ = 2.4 Hz, 1H, Ar-H), 7.36 (d, $^{4}J_{HH}$ = 2.6 Hz, 1H, Ar-H), 8.38 (s, 1H, N=CH), 14.07 (s, 1H, OH).

2.3.3 Synthesis of HL3[23]

A mixture of 3,5-di-*tert*-butyl-2-hydroxybenzaldehyde (2.35 g, 10.0 mmol), 2,4,6-trimethylaniline (2.63 g, 10.0 mmol) and *p*-toluene sulfonic acid (0.351 g, 1.82 mmol) in ethanol (100 mL) was refluxed for 48 h. The precipitate was collected using suction filtration (2.30 g, 10.0 mmol, 66%) and recrystallized in wet and dry dichloromethane, yielding a yellow crystalline product. ^{1}H NMR ($CDCl_3$, ppm): δ = 1.34 [s, 9H, $C(CH_3)_3$], 1.50 [s, 9H, $C(CH_3)_3$], 2.19 (s, 6H, CH_3), 2.30 (s, 3H, CH_3), 6.92 (s, 2H, Ar-H) 7.14 (d, $^{4}J_{HH}$ = 2.6 Hz, 1H, Ar-H), 7.48 (d, $^{4}J_{HH}$ = 2.4 Hz, 1H, Ar-H), 8.33 (s, 1H, CH=N), 13.58 (s, 1H, OH).

2.4 Synthesis of [Na(L)]

2.4.1 Synthesis of NaL1

Under N_2 atmosphere, a solution of **HL1** (0.17 g, 0.57 mmol) in THF (5 mL) was added dropwise to a solution of sodium hydride (30.0 mg, 1.25 mmol) in THF (5 mL) cooled to -78°C. The reaction mixture turned yellow and became cloudy. The solution was left to warm to room temperature and stir for 18 h.

2.4.2 Synthesis of NaL2

Under N_2 atmosphere, a solution of **HL2** (0.17 g, 0.54 mmol) in THF (5 mL) was added dropwise to a solution of sodium hydride (30.0 mg, 1.25 mmol) in THF (5 mL) cooled to -78°C. Upon this addition, the reaction mixture turned yellow and became cloudy. The solution was left to warm to room temperature and stir for 18 h.

2.4.3 Synthesis of NaL3

Under N_2 atmosphere, a solution of **HL3** (0.18 g, 0.51 mmol) in THF (5 mL) was added dropwise to a solution of sodium hydride (30.0 mg, 1.25 mmol) in THF (5 mL) cooled to -78°C. Upon this addition, the reaction mixture turned yellow and became cloudy. The solution was left to warm to room temperature and stir for 18 h.

2.5 Synthesis of Me_2BiBr[24]

Under N_2 atmosphere, methyllithium (1.6 M in Et_2O, 8.4 mL, 13.4 mmol) was added dropwise to a solution of bismuth(III) bromide (3.00 g, 6.69 mmol) in ethyl ether (75 mL) cooled to -78°C. The reaction mixture was left to warm to room temperature and stir for 18 h, where a white precipitate was produced. The mixture was filtered and the filtrate was concentrated *in vacuo* to 40 mL. Hexanes (40 mL) was added and the product began to precipitate. The solvent was removed *in vacuo* and the off-white product was collected (2.32 g, 7.28 mmol, 85%). ^{1}H NMR ($CDCl_3$, ppm): δ = 2.01 (s, 6H, CH_3).

2.6 Synthesis of [(L)$BiMe_2$]

2.6.1 Attempted Synthesis of [(L1)$BiMe_2$] (1)

Under N_2 atmosphere, **Me_2BiBr** (0.18 g, 0.57 mmol) in THF (5 mL) was added to the previously prepared **NaL1** solution (0.17 g, 0.57 mmol). The resulting solution was yellow and became cloudy. After stirring for 18 h, the reaction mixture was filtered and the clear yellow solution was concentrated to 1 mL and stored at -15°C overnight. The yellow powder that precipitated was collected by filtration and characterized by ^{1}H NMR spectroscopy, which indicated that the product was a mixture of product and ligand. It was determined that **1** could be generated *in situ*, but upon recrystallization the reprotonated ligand was isolated.

2.6.2 Attempted Synthesis of [(L2)BiMe$_2$] (2)

Under N_2 atmosphere, **Me$_2$BiBr** (0.17 g, 0.54 mmol) in THF (5 mL) was added to the previously prepared **NaL2** solution (0.17 g, 0.54 mmol). The resulting solution was yellow and became cloudy. After stirring for 18 h, the reaction mixture was filtered and the clear yellow solution was concentrated to 1 mL and stored at -15°C overnight. The yellow powder that precipitated was collected by filtration and characterized by ^{1}H NMR spectroscopy, which indicated that the product was a mixture of product and ligand. The target complex **2** was generated *in situ*, however, upon recrystallization, the reprotonated ligand could only be isolated

2.6.3 Attempted Synthesis of [(L3)BiMe$_2$] (3)

Under N_2 atmosphere, **Me$_2$BiBr** (0.16 g, 0.51 mmol) in THF (5 mL) was added to the previously prepared **NaL3** solution (0.18 g, 0.54 mmol). The resulting solution was yellow and became cloudy. After stirring for 18 h, the reaction mixture was filtered and the clear yellow solution was concentrated to 1 mL and stored at -15°C overnight. Yellow crystals precipitated from the solution, which were collected by filtration. ^{1}H NMR and FT-Raman spectra indicated that the product was a mixture of product and ligand. The target complex **3** was generated *in situ*, but upon recrystallization, only the reprotonated ligand was isolated.

2.7 Synthesis of [(L)InMe$_2$]

2.7.1 Synthesis of [(L1)InMe$_2$] (4)

Under N_2 atmosphere, **HL1** (0.20 g, 0.69 mmol) in THF (2 mL) was added dropwise to a solution of trimethylindium (0.11 g, 0.69 mmol) in THF (2 mL), where bubbling occurred. The yellow reaction mixture was left to stir for 3 h then was left to sit at 23°C for 24 h, which resulted in precipitation of a powder product (0.24 g, 0.55 mmol, 60%). Mp 80.0 – 86.7 °C.

FT-IR (cm^{-1}): 2952m (C-H stretch), 1612s (C=N stretch), 1532m, 1462w, 1434w, 1409w, 1361w, 1323w, 1256w, 1236w, 1160s, 1023w, 978w, 906w, 879w, 838m, 785m, 746w, 712m, 637w. FT-Raman (cm^{-1}): 2967m (C-H stretch), 2920m (Ar-CH), 1612m (C=N stretch), 1533w, 1460w, 1436m, 1345w, 1237vw, 1200vw, 1157w, 924w, 839vw, 550w, 519w, 486s [ν_{sym} (Me-In-Me)], 229w, 127s. ^{1}H NMR ($CDCl_3$, ppm): δ = -0.107 (s, 6H, CH_3), 1.30 [s, 9H, $C(CH_3)_3$], 1.40 [d, J = 2.6 Hz, 18H, $C(CH_3)_3$], 6.86 (d, $^{4}J_{HH}$ = 2.8 Hz, 1H, Ar-H), 7.41 (d, $^{4}J_{HH}$ = 2.8 Hz, 1H, Ar-H), 8.13 (s, 1H, N=CH). $^{13}C\{^{1}H\}$ NMR ($CDCl_3$, ppm): -5.1 (In-CH_3), 29.4 [C(CH_3)], 31.5 [C(CH_3)], 34.6 [$C(CH_3)$], 34.6 [$C(CH_3)$], 56.8 [NAr-$C(CH_3)$], 59.2 [NAr-C(CH_3)], 118.2 (all Ar-C), 125.9, 128.6, 130.1, 135.6, 141.3, 160.6, 166.3, 167.9 (CH=N).

2.7.2 Synthesis of [(L2)InMe$_2$] (5)

Under N_2 atmosphere, **HL2** (0.27 g, 0.87 mmol) in diethyl ether (2 mL) was added dropwise to a solution of trimethylindium (0.14 g, 0.87 mmol) in diethyl ether (2 mL), where bubbling occurred. The yellow reaction mixture was left to stir for 3 h and concentrated to 2 mL *in vacuo*. This resulted in precipitation of a crystalline product that was collected by filtration (0.16 g, 0.35 mmol, 54%). Mp 149–152 °C. FT-IR (cm^{-1}): 2946m (C-H stretch), 2922m, 2852m, 1611s (C=N stretch), 1547w, 1532m, 1460w, 1419m, 1384w, 1361w, 1326m, 1255w, 1198w, 1167s, 1075s, 1027w 838w, 785m, 747w, 717m, 635m. FT-Raman (cm^{-1}): 2945m (C-H stretch), 2924m, 2854w, 1611s (C=N stretch), 1533m, 1460w, 1436m, 1349w, 1260vw, 1238vw, 1201vw, 1156w, 1074vw, 919w, 845vw, 797w, 631w, 552w, 521w, 488s [ν_{sym} (Me-In-Me)], 380vw, 303vw, 210m, 127s. ^{1}H NMR ($CDCl_3$, ppm): δ = -0.13 (s, 6H, CH_3), 1.22–1.55 (m, 10H, cyclohexyl-H) 1.27 [s, 9H, $C(CH_3)_3$], 1.39 [s, 9H, $C(CH_3)_3$], 3.13 (m, 1H, cyclohexyl-H), 6.81 (d, $^{4}J_{HH}$ = 2.8 Hz, 1H, Ar-H), 7.40 (d, $^{4}J_{HH}$ = 2.8 Hz, 1H, Ar-H), 8.06 (s, 1H, N=CH). $^{13}C\{^{1}H\}$ NMR ($CDCl_3$, ppm): -5.3 (In-CH_3), 25.1 (C_6H_{11}), 29.4 [C(CH_3)], 31.4

[C(CH_3)], 34.9 [C(CH_3)], 35.4 [C(CH_3)], 71.0, 117.9 (all Ar-C), 125.3, 128.6, 129.9, 135.6, 141.3, 166.9, 169.6 (CH=N).

2.7.3 Synthesis of [(L3)InMe$_2$] (6)

Under N_2 atmosphere, HL3 (0.27 g, 0.87 mmol) in toluene (2 mL) was added dropwise to trimethylindium (0.13 g, 0.81 mmol) in toluene (2 mL), where bubbling occurred. The yellow reaction mixture was left to stir for 3 h, concentrated *in vacuo* to ~2 mL and stored at -15°C. After 48 h, a crystalline product precipitated and was collected by filtration (0.15 g, 0.31 mmol, 48%). Mp 131–134 °C. FT-IR (cm^{-1}): 2948m (C-H stretch), 1597s (C=N stretch), 1526s, 1459m, 1425m, 1382w, 1323m, 1253m, 1160w, 1132s, 980m, 848w, 831w, 718m, 675m, 634w. FT-Raman (cm^{-1}): 2922m (C-H stretch), 1598s (C=N stretch), 1528m, 1459m, 1426s, 1380w, 1343m, 1303vw, 1209w, 1158w, 1133m, 916w, 626w, 576w, 524w, 484s [ν_{sym} (Me-In-Me)], 314vw, 192w, 153m, 134m. ^{1}H NMR ($CDCl_3$, ppm): δ = -0.138 (s, 6H, CH_3), 1.28 [s, 9H, C(CH_3)$_3$], 1.43 [s, 9H, C(CH_3)$_3$], 2.18 (s, 6H, CH_3), 2.29 (s, 3H, CH_3), 6.83 (d, $^4J_{HH}$ = 2.8 Hz, 1H, Ar-H), 6.92 (s, 2H, Ar-H), 7.48 (d, $^4J_{HH}$ = 3.0 Hz, 1H, Ar-H), 7.87 (s, 1H, N=CH). ^{13}C{^{1}H} NMR ($CDCl_3$, ppm): -5.5 (In-CH$_3$), 18.5 (NAr-CH$_3$), 20.8 (NAr-CH$_3$), 29.4 [C(CH$_3$)], 31.3 [C(CH$_3$)], 33.8 [C(CH_3)], 35.5 [C(CH_3)], 117.9 (all Ar-C), 125.3, 130.3, 135.6, 141.8, 145.5, 167.7, 173.8 (CH=N).

2.8 X-Ray Crystallography

Crystals of **5** and **6** were isolated and analyzed by X-ray crystallography. A crystal of compound **HL3**, **5** and **6** was mounted from Paratone-N oil on a MiTeGen MicroMount. The data were collected on a Bruker APEX II charge-coupled-device (CCD) diffractometer, with an Oxford 700 Cryocool sample cooling device. The instrument was equipped with graphite-monochromated Mo Kα radiation (λ = 0.71073 Å; 30 mA, 50 mV), with MonoCap X-ray

source optics. For data collection, four ω-scan frame series were collected with 0.5° wide scans, 5 second frames and 366 frames per series at varying φ angles (φ = 0°, 90°, 180°, 270°). Data collection, unit cell refinement, data processing and multi-scan absorption correction were applied using the APEX2[25] or APEX3[26] software packages. The structures were solved using SHELXT[27] and all non-hydrogen atoms were refined anisotropically with SHELXL[28] using a combination of shelXle[29] and OLEX2[30] graphical user interfaces. Unless otherwise noted, all hydrogen atom positions were idealized and ride on the atom to which they were attached. The final refinement included anisotropic temperature factors on all non- hydrogen atoms. Details of crystal data, data collection, and structure refinement are listed in Table 1.

Table 1. Crystallographic data for **HL3**, **5** and **6**.

	HL3	**5**	**6**
formula	$C_{24}H_{33}NO$	$C_{23}H_{38}InNO$	$C_{26}H_{38}InNO$
fw	351.51	459.36	495.39
crystal system	orthorhombic	monoclinic	monoclinic
space group	*Pbca*	$P2_1/n$	$P2_1$
a (Å)	9.993(14)	11.8445(9)	12.341(2)
b (Å)	11.992(17)	9.154(7)	8.688(17)
c (Å)	35.926(5)	21.4357(17)	12.874(3)
α (deg)	90	90	90
β (deg)	90	91.748(10)	113.828(2)
γ (deg)	90	90	90
V ($Å^3$)	4305.1(10)	2323.0(3)	1262.6(4)
Z	8	4	2
F*(000)*	1536	960	516
ρ_{calcd}, $g\ cm^{-3}$	1.085	1.313	1.303
μ, mm^{-1}	0.07	1.03	0.95
T, K	293(2)	421(2)	125(2)
λ, Å	0.71073	0.71073	0.71073
R_1 [a]	0.046	0.032	0.038
wR_2 [b]	0.097	0.066	0.065

[a] $R_1 = [\Sigma||F_o|-|F_c||]/[\Sigma|F_o|]$ for $[F_o^2 > 2\sigma(F_o^2)]$. [b] $wR_2 = \{[\Sigma w(F_o^2 - F_c^2)^2]/[\Sigma w(F_o^4)]\}^{½}$.

3. Results and Discussion

3.1 Synthesis of Phenoxy-imine Ligands

The three target phenoxy-imine ligands were synthesized by a condensation reaction according to methods adapted from procedures previously published in the literature (Scheme 2).[22,23] The three reactions used 3,5-di-*tert*-butyl-2-hydroxybenzaldehyde and a primary amine as reactants. For **HL1** and **HL2**, methanol was used as the solvent, while ethanol was used for **HL3**. The aldehyde was added to the solvent and the corresponding primary amine was added, yielding a yellow solution for all three ligand preparations. The **HL1** and **HL2** reaction mixtures stirred for 24 h and the **HL3** reaction was heated at reflux for 48 h. The products were collected and achieved yields of 79%, 89% and 66%, respectively.

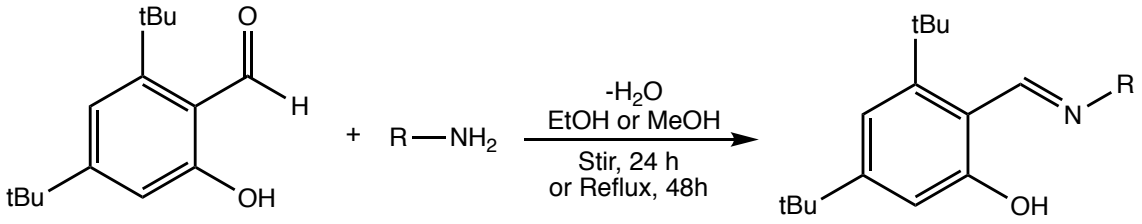

HL1, R = tBu **HL2**, R = cyclohexyl **HL3**, R = 2,4,6-$Me_3C_6H_2$

Scheme 2. General synthesis of phenoxy-imine ligands.

The **HL1** solution began to precipitate after 1 h of stirring, and after the 24 h the reaction vessel contained a cloudy yellow reaction mixture. The yellow solid was collected by suction filtration and gave a powder product that was washed with methanol and dried *in vacuo* for 1 h. Solubility tests for **HL1** determined it to be soluble in diethyl ether, THF, toluene, hexanes and dichloromethane. The crude product was characterized by ^{1}H NMR spectroscopy, which showed the equivalent spectroscopic data as the previously reported literature values (Appendix 1).[22] The crude material was recrystallized in wet and dry dichloromethane, which

yielded clear yellow crystals. The recrystallized **HL1** was characterized again by ^{1}H NMR to obtain a cleaner spectrum.

Comparably to **HL1**, a yellow precipitate was observed after 1 h of stirring for the **HL2** reaction mixture. After 24 h of stirring, the yellow solid was collected by suction filtration and gave a powder product that was washed with methanol and dried *in vacuo* for 1 h. **HL2** was determined to be soluble in diethyl ether, THF, toluene, hexanes and dichloromethane. The crude product was characterized by ^{1}H NMR spectroscopy, which showed the same spectroscopic data as the previously reported literature values (Appendix 2).[22] **HL2** was recrystallized in wet and dry dichloromethane, which resulted in a yellow crystalline product. A second ^{1}H NMR spectrum was taken to obtain a cleaner spectrum.

Throughout the duration of the 48 h reflux for the synthesis of **HL3**, no precipitation occurred. The reaction mixture was then cooled to room temperature and was then placed in an ice bath where precipitation of a yellow crystalline product occurred almost immediately. Solubility testing for **HL3** determined that it is soluble in diethyl ether, THF, toluene, hexanes and dichloromethane. ^{1}H NMR spectroscopy data was obtained and compared to previously reported literature values, determining that the desired structure was achieved (Appendix 3).[23] Recrystallization of **HL3** was carried out in both wet and dry dichloromethane, yielding yellow crystals. The recrystallized ligand was characterized again by ^{1}H NMR spectroscopy to obtain a cleaner spectrum.

3.2 Deprotonation of Phenoxy-imine Ligands

The deprotonation of the three target ligands, **HL1**, **HL2** and **HL3**, was successful and resulted in formation of **NaL1**, **NaL2** and **NaL3** (Scheme 3). The deprotonation reactions took place under N_2 atmosphere and the process was similar for each ligand. The **HL** solution was

placed cooled to -78°C. An excess amount of sodium hydride (1.5 equiv.) was used to ensure the ligands fully deprotonated; however, the sodium hydride did not fully dissolve into the THF. For all reactions, the sodium hydride solution was transferred to the ligand solution using Schlenk line techniques. Upon its addition, the reaction mixture became immediately cloudy and was yellow in colour. Following 18 h of stirring, deprotonation was confirmed by ^{1}H NMR spectroscopy for each ligand (Appendices 4, 5, 6). The disappearance of the hydroxyl hydrogen peak, between 13.58 and 14.59 ppm, in the ^{1}H NMR spectrum indicated a successful deprotonation. It was later determined that deprotonation occurred after 3 h of stirring, resulting in a more time and energy efficient method.

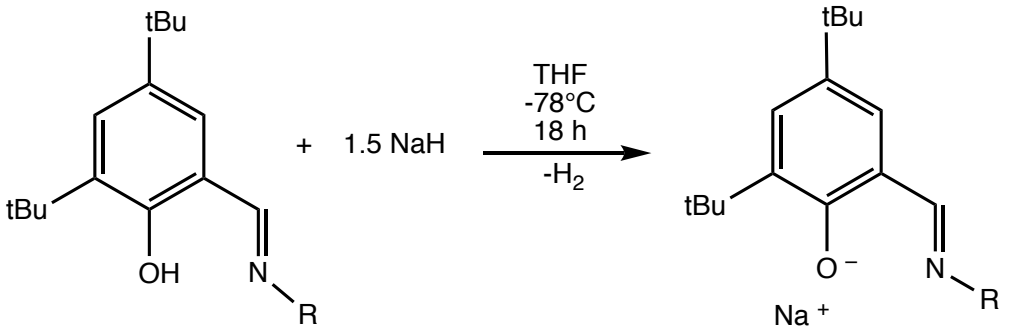

L1, R = tBu **L2**, R = cyclohexyl **L3**, R = 2,4,6-$Me_3C_6H_2$

Scheme 3. General phenoxy-imine ligand deprotonation reaction.

Although deprotonation was achieved for all three ligands, it was not always successful. Initially, one equivalent of sodium hydride was used to deprotonate the ligand, but this proved to be unsuccessful. As sodium hydride is not very soluble in THF, not all was being transferred to the ligand solution, which also contributed to the lack of deprotonation observed for some reactions. To circumvent this issue, the ligand solution was instead added to the sodium

hydride slurry that was cooled to -78°C. This procedural adaptation produced a more successful method of ligand deprotonation.

3.3 Synthesis of Me_2BiBr

Dimethylbismuth bromide (**Me_2BiBr**) has been chosen as a starting material in the metathesis reaction for bismuth complexation instead of trimethylbismuth. This decision was based upon the previous finding that trimethylbismuth is very unstable and unreactive. The methods for synthesizing **Me_2BiBr** were adapted from a published procedure (Scheme 4).[24] The addition of bismuth(III) bromide to diethyl ether was carried out under N_2 atmosphere and was a clear, colourless solution. The bismuth solution was cooled to -78°C before the dropwise addition of 1.6 M methyl lithium. The reaction was left to stir for 18 h, where a grey precipitate, indicative of elemental bismuth, formed. The solution was filtered and the resulting clear filtrate was concentrated *in vacuo* to half of the original volume. Hexane was added with the goal of reducing the solubility of the product and, therefore, inducing precipitation. A powder solid precipitated and the solvent was removed *in vacuo*. Prior to a successful synthesis of **Me_2BiBr**, a solid product could not be obtained or the product would degrade. These problems were partly associated with the literature preparations that were being followed. Therefore, the methods were adapted, which resulted in consistent production of Me_2BiBr. The procedural alterations involved using hexanes to induce precipitation and allowing a longer stir period than the 30-minute period published in the literature. Attempts to recrystallize the product were unsuccessful. The ^{1}H NMR spectroscopic data of the **Me_2BiBr** powder was relatively clean (Appendix 7) and the product was used for further reactions.

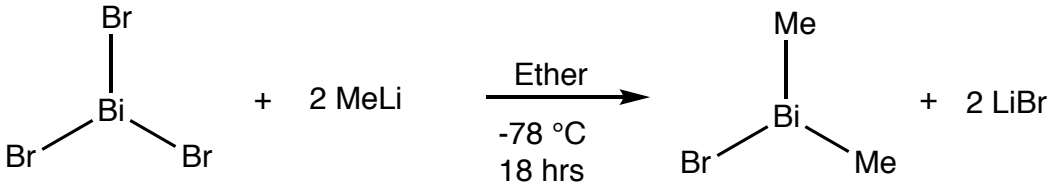

Scheme 4. Synthesis of **Me_2BiBr**.

3.4 Synthesis of [(L)$BiMe_2$]

Syntheses of the target bismuth complexes **1**, **2** and **3** were attempted using a metathesis reaction of **NaL** and **Me_2BiBr** under N_2 atmosphere. The **Me_2BiBr** did not dissolve very well in THF, so the **NaL** solution was added to the former. Upon the addition of **Me_2BiBr**, all three reaction mixtures turned cloudy yellow immediately. Following 18 h of stirring, the solution was filtered to remove the white salt precipitate. Initially, the solutions were concentrated to half of the original volume *in vacuo* and left at -15°C overnight.

3.4.1 Attempted Synthesis of [(L1)$BiMe_2$] (1)

After leaving the **[(L1)$BiMe_2$] (1)** solution at -15°C overnight, precipitation of a yellow powder was observed. The solvent was removed and the resulting yellow solid was characterized by ^{1}H NMR spectroscopy. According to the spectra, the OH peak at 14.66 ppm was still present, indicating reformation of **HL1**. The product did not form, which could be attributed to a number of different factors. In response to a few failed attempts, **HL1** was recrystallized again in dry dichloromethane and anhydrous sodium sulfate was used to help dry the ligand solution. The recrystallized dry ligand was used in following metathesis reactions. According to ^{1}H NMR spectroscopic analysis of subsequent attempts indicated that a mixture of product and ligand had precipitated (Appendix 8). Various solvents were used, with the goal of isolating the target complex and yielding a crystalline material. The precipitate

was soluble in THF, toluene and hexanes, slightly soluble in pentane and insoluble in diethyl ether. Crystals were isolated from toluene, however, spectroscopic analysis indicated that the product had reacted with residual moisture and to yield **HL1**. Throughout the attempted syntheses of **1**, water contamination was a difficult problem to circumvent regardless of the precautions that were taken to ensure that the reaction was completely anhydrous. This demonstrates that the target complex is very moisture sensitive and although the compound can be made *in situ*, it is too hydrolytically unstable to isolate.

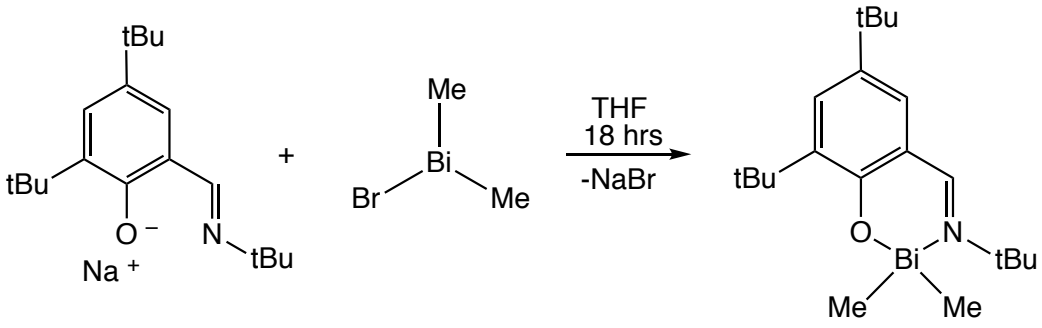

Scheme 5. Synthesis of **1**.

3.4.2 Attempted Synthesis of [(L2)BiMe$_2$] (2)

For the first attempt at synthesizing **[(L2)BiMe$_2$] (2)** a yellow precipitate precipitated from solution after sitting at -15°C overnight. Comparably to **1**, the powder was characterized by ^{1}H NMR spectroscopy, which indicated that only **HL2** was present. Following a few failed attempts, the ligand was dried using anhydrous sodium sulfate and was then recrystallized in wet and dry dichloromethane. For subsequent synthesis attempts, ^{1}H NMR spectra of the **2** reaction mixtures indicated that the target bismuth compound was formed in a mixture with the ligand (Appendix 9). The product obtained was soluble in THF, pentane, diethyl ether and slightly soluble in toluene and hexanes. It is proposed that due to the hydrolytic instability of the Bi–O bond in the target complex, the compounds underwent reaction with residual

moisture during recrystallization and only **HL2** could be isolated.

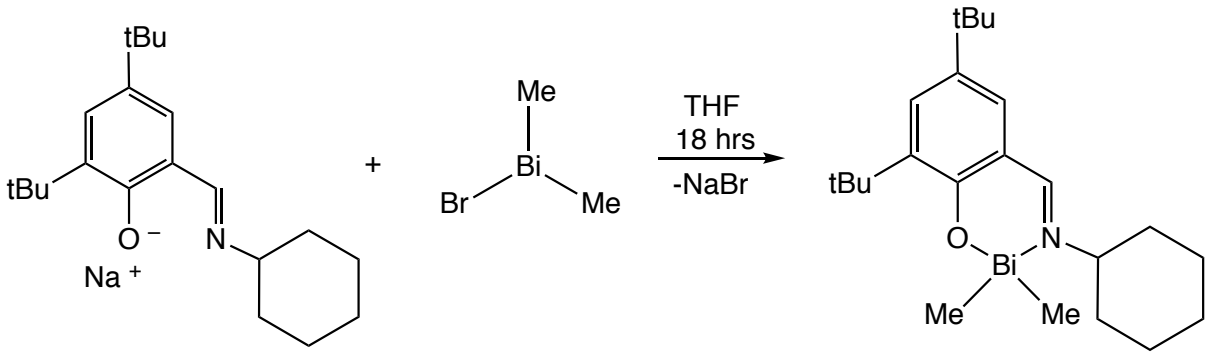

Scheme 6. Synthesis of **2**.

2.4.3 Attempted Synthesis of [(L3)BiMe$_2$] (3)

After leaving the **[(L3)BiMe$_2$] (3)** solution at -15°C overnight, the mixture was further concentrated resulting it immediate precipitation of product. The solution was filtered and again allowed to sit at -15°C. After one week crystals had formed. ^{1}H NMR (Appendix 10) and FT-Raman spectroscopy (Appendix 11) confirmed that the target product **3** had precipitated. However, the crystals that formed at -15°C redissolved as the solution returned to room temperature. Another attempt yielded well-formed crystals that were analyzed by X-ray crystallography. The data from the analysis produced an X-ray crystal structure of **HL3** (Figure 13). The crystal structure has been included to emphasize the notion that these bismuth complexes are very moisture sensitive and result in the isolation of reprotonated ligand upon recrystallization.

After many attempts, it was determined from ^{1}H NMR spectra of reaction mixtures that all three target bismuth complexes **1**, **2** and **3** were formed *in situ*. However, the spectra indicate a mixture of product and ligand in the reaction mixtures and isolation of only the reprotonated phenoxy-imine ligands upon recrystallization. These findings of moisture

sensitivity in bismuth alkoxide species are in line with what has been previously published in the literature.[8]

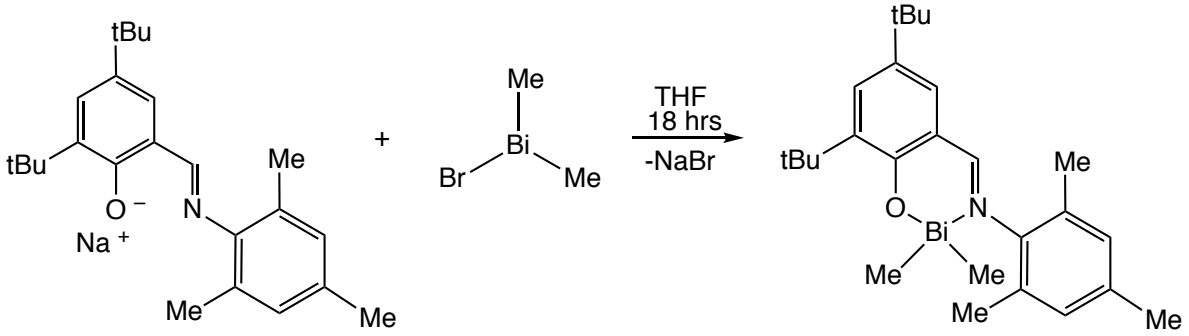

Scheme 7. Synthesis of **3**.

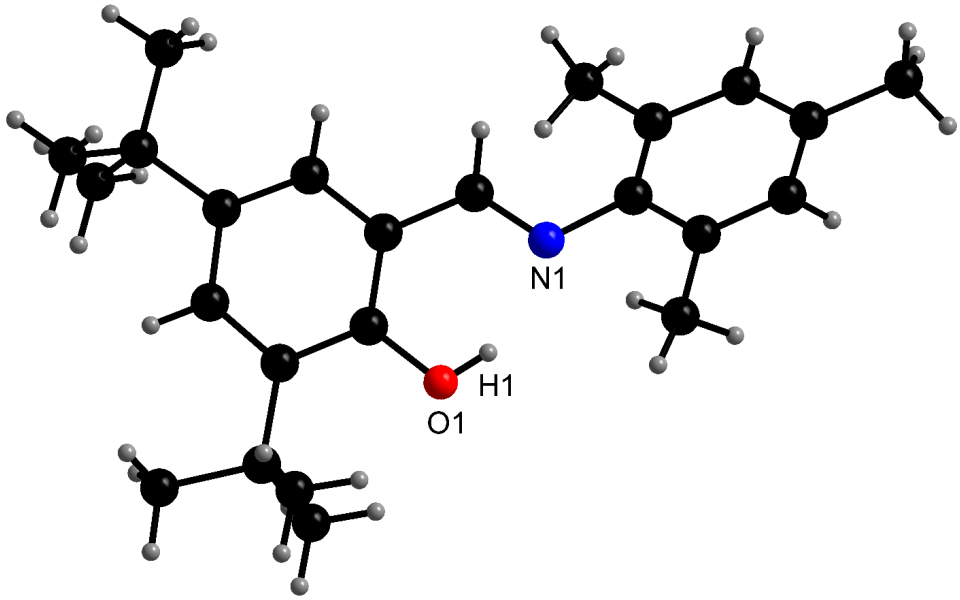

Figure 13. X-ray crystal structure of **HL3**.

3.5 Synthesis of [(L)InMe$_2$]

The indium target complexes **4**, **5**, and **6** were synthesized using trimethylindium and **HL** under N_2 atmosphere. The first solvent that was used for these reactions was THF. Trimethylindium was dissolved in THF and the ligand was dissolved in THF in another vial.

Upon the addition of a solution of ligand to a solution of trimethylindium, bubbling began to occur. Bubbling throughout the 3 h period of stirring is indicative of the release of methane gas (Schemes 8, 9, 10). For the synthesis of **4**, **5**, and **6**, the yellow reaction mixtures were left to stir for 3 h.

3.5.1 Synthesis of [(L1)InMe$_2$] (4)

The **[(L1)InMe$_2$] (4)** reaction mixture was concentrated *in vacuo* to a volume of ~2 mL and was left at -15°C overnight. Over the course of 48 h no precipitate was observed. Therefore, different solvents were tested for solubility and used in this reaction. Following the initial use of THF, the reaction was repeated in hexanes, toluene, and diethyl ether. A yellow powder precipitate was obtained using diethyl ether. ^{1}H NMR spectroscopy was used to characterize the product, which determined to be the target compound **4**. The spectrum shows a peak at -0.11 ppm, which is attributed to the *Me$_2$*In hydrogen atoms. Crystals of the compound have not yet been obtained. Therefore, characterization of **4** by mp, ^{1}H NMR (Appendix 12) and ^{13}C{^{1}H} NMR spectroscopy (Appendix 13), FT-Raman spectroscopy (Appendix 14), and FT-IR spectroscopy (Appendix 15) has been carried out using the powder product.

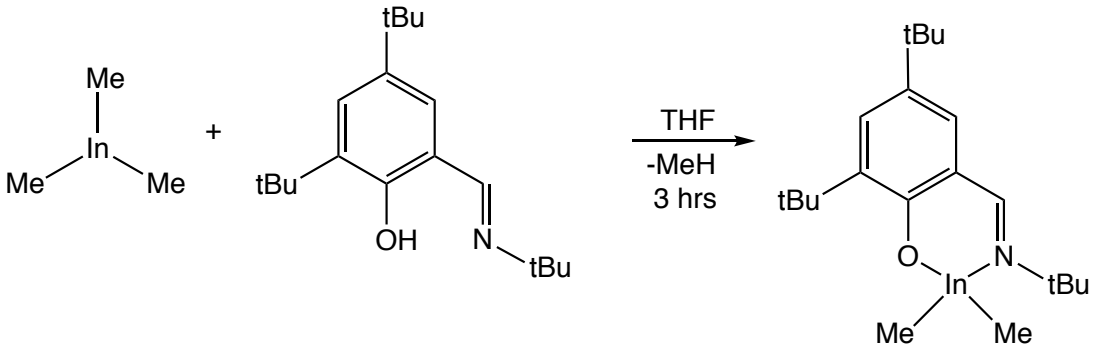

Scheme 8. Synthesis of **4**.

3.5.2 Synthesis of [(L2)InMe$_2$] (5)

After concentrating the **[(L2)InMe$_2$] (5)** reaction mixture *in vacuo* to ~3 mL and no precipitate was observed. The solution was left at room temperature overnight, which resulted in a small amount of yellow solid precipitate. The mixture was filtered to remove the solid and was then concentrated to ~1 mL. The clear yellow solution was stored at -15°C overnight. The powder that was collected was characterized by ^{1}H NMR spectroscopy, confirming that **5** had formed. With the goal of obtaining crystals for this compound, different solvents were tested. Compound **5** is soluble in THF, hexanes, diethyl ether and toluene.

In an attempt at growing crystals, diethyl ether was used as the reaction solvent. Following the 3 h stir, the reaction mixture was concentrated *in vacuo* and upon which formation of clear yellow crystals of the product occurred almost immediately. The crystalline product **5** has been characterized by mp, ^{1}H NMR (Appendix 16) and ^{13}C{^{1}H} NMR spectroscopy (Appendix 17), FT-Raman spectroscopy (Appendix 18), FT-IR spectroscopy (Appendix 19), and X-ray crystallography (Figure 14).

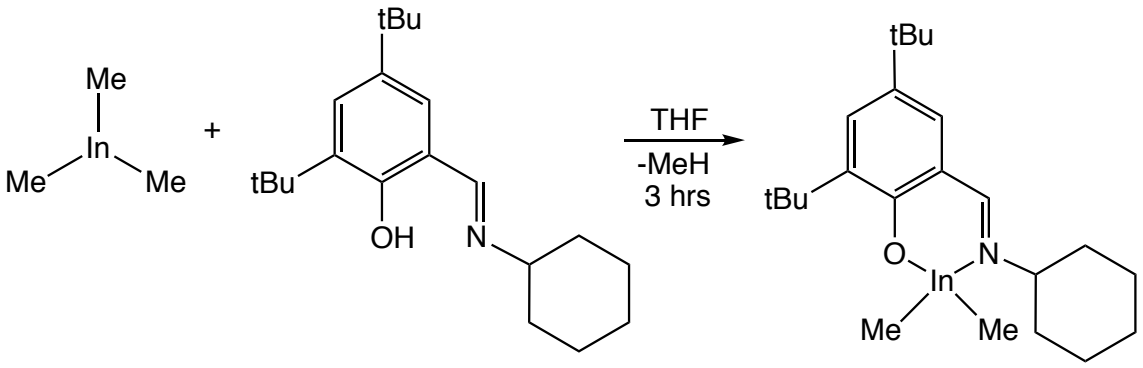

Scheme 9. Synthesis of **5**.

3.5.3 Synthesis of [(L3)InMe$_2$] (6)

The **[(L3)InMe$_2$] (6)** reaction mixture was concentrated to ~1 mL *in vacuo* and was left at -15°C overnight. No precipitation was observed using THF as the solvent. Therefore, the use of other solvents was explored. THF, hexanes, toluene or diethyl ether were also used as the reaction solvent. When diethyl ether was used as a solvent, the reaction mixture was concentrated to ~3 mL after the 3 h of stirring. The solution was left at room temperature overnight, which resulted in precipitation of a yellow powder. ^{1}H NMR spectroscopy confirmed that **6** has been isolated.

With a goal of obtaining a crystalline product, the reaction was repeated in toluene. Following the 3 h of stirring, the reaction mixture was concentrated to ~2 mL *in vacuo* and was stored at -15°C overnight. No precipitate was observed; therefore, the reaction mixture was concentrated further to ~1 mL and was left at -15°C overnight. This resulted in precipitation of crystals. The crystalline product, **6**, has been characterized by mp, ^{1}H NMR (Appendix 20) and ^{13}C{^{1}H} NMR spectroscopy (Appendix 21), FT-Raman spectroscopy (Appendix 22), FT-IR spectroscopy (Appendix 23), and X-ray crystallography (Figure 14).

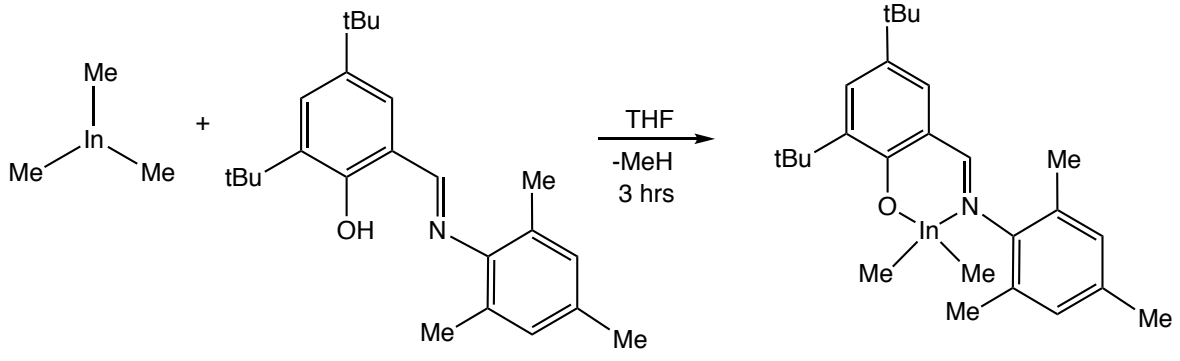

Scheme 10. Synthesis of **6**.

3.6 X-Ray Crystal Structures

Suitable crystals were analyzed by X-ray crystallography for **5** and **6**. The bond distances and angles are given in Table 2. The crystal structure of **5** shows the four coordination sites on indium that are occupied by two Me groups [In1-C1 = 2.142(3) Å, In1-C2 = 2.145(2) Å]. The indium centre is also coordinated to an O atom [In1-O1 = 2.096(2) Å] and a N atom [In1-N1 = 2.232(2)]. The bond angles of **5** suggest a distorted tetrahedral geometry [C1-In1-C2 = 132.3(9), N1-In1-O1 = 86.6(7)]. The crystal structure of **5** confirms the formation of the target dimethylindium phenoxy-imine complex.

Comparably to **5**, the crystal structure for complex **6** shows the four coordination sites on indium that are occupied by two Me groups [In1-C1 = 2.141(4) Å, In1-C2 = 2.138(6) Å], an O atom [In1-O1 = 2.094(4) Å] and a N atom [In1-N1 = 2.237(4)]. The bond angles given for **6** also suggest a distorted tetrahedral geometry at the indium centre [C1-In1-C2 = 138.2(2), N1-In1-O1 = 84.3(1)]. The crystal structure of **6** confirms the formation of another target dimethylindium phenoxy-imine complex.

The crystal structures of **5** and **6** can be compared to the previously reported aluminum analogues that are catalytically active for the ROP of cyclic esters. Figure 10 shows a series of phenoxy-imine supported aluminum catalysts with derivatives similar to **5** and **6**. The overall shape of the indium complexes and geometry at the metal centre are comparable to aluminum analogues.[31] However, the bond distances for the aluminum complexes are shorter than the equivalent bonds in the indium complexes. This is expected as the atomic radius of aluminum is smaller than that of indium.

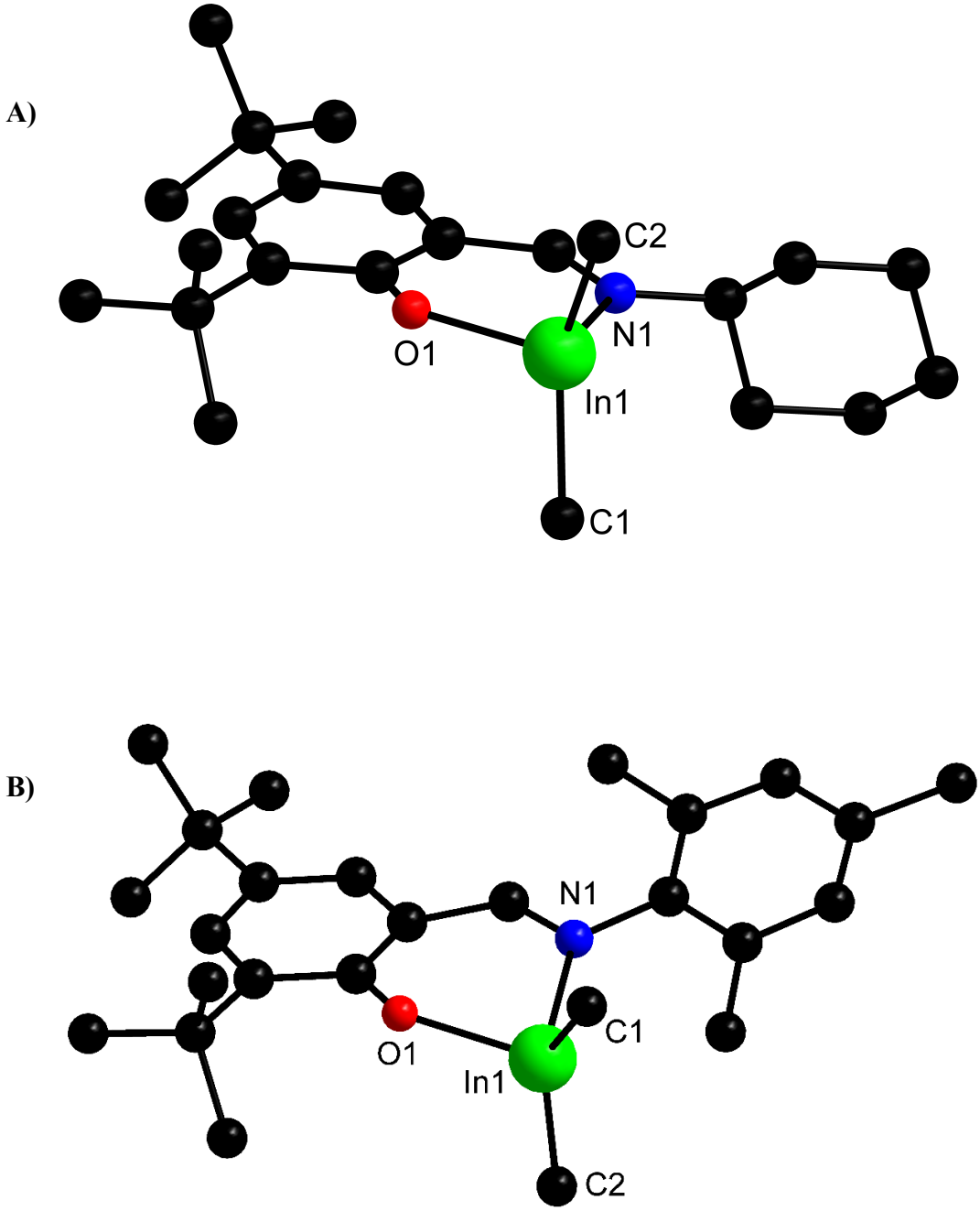

Figure 14. X-ray crystal structures of A) **5** and B) **6**.

Table 2. Selected bond distances (Å) and angles (˚) for **5** and **6**.

	5	**6**
In1-C1	2.142(3)	2.141(4)
In1-C2	2.145(2)	2.138(6)
In1-O1	2.096(2)	2.094(4)
In1-N1	2.232(2)	2.237(4)
C1-In1-C2	132.3(9)	138.2(2)
N1-In1-O1	86.6(7)	84.3(1)

4. Conclusion

The aim of this study was to synthesize and characterize novel dimethylbismuth and -indium phenoxy-imine complexes for the ROP of cyclic esters. The three phenoxy-imine ligand compounds **HL1**, **HL2** and **HL3** and the **Me_2BiBr** were successfully isolated and characterized by ^{1}H NMR spectroscopy. The *in situ* deprotonation of the ligands to **NaL** was a successful step in the bismuth complexation reaction, which was confirmed by the absence of the hydroxyl hydrogen peak in the ^{1}H NMR spectrum.

The metathesis reaction that was proposed for the deprotonated ligands and **Me_2BiBr** was a promising method for synthesizing the target bismuth compounds (**1**, **2**, and **3**). However, issues of water contamination were a problem throughout the attempted bismuth complexation reactions. ^{1}H NMR spectra of the products yielded from these reactions indicate that **1**, **2**, and **3** have been formed *in situ*. However, upon recrystallization only the reprotonated ligands were isolated due to the hydrolytic instability of the Bi–O bond in the target bismuth complexes.

The synthesis of phenoxy-imine supported indium complexes **4**, **5**, and **6** was successful. The three indium complexes were characterized by mp, ^{1}H NMR and $^{13}C\{^{1}H\}$ NMR spectroscopy, FT-IR spectroscopy, and FT-Raman spectroscopy. Crystals of complexes **5** and **6** have been isolated and analyzed by X-ray crystallography.

5. Future Directions

The synthesis of bismuth alkoxide species investigated could be revisited using different phenoxide ligands. However, attempts at making these compounds were fairly exhaustive and significant attempts to eliminate moisture were undertaken. Crystals should be obtained for compound **4** and analyzed by X-ray crystallography. The isolated indium products can be screened as catalysts for the ROP of cyclic esters and their performance can be compared to their aluminum counterparts that have been previously reported in the literature. The scope of the study can be broadened by further varying the ligand steric bulk to change the reactivity of these complexes and compare the results to previously studied ROP catalysts.

6. References

[1] Anastas, P.; Eghbali, N. Green Chemistry: Principles and Practice. *Chem. Soc. Rev.* **2010**, *39*, 301-312.

[2] A. Sheldon, R. The E Factor 25 Years on: The Rise of Green Chemistry and Sustainability. *Green Chem.* **2017**, *19*, 18-43.

[3] Thompson, R.C.; Moore, C.J.; Vom Saal, F.S.; Swan, S.H. Plastics, the Environment and Human Health: Current Consensus and Future Trends. *Philo. Trans. Roy. Soc. B: Bio. Sci.* **2009**, *364*, 2153-2166.

[4] Iwata, T. Biodegradable and Bio-based Polymers: Future Prospects of Eco-Friendly Plastics. *Angew. Chem. Int. Ed.* **2015**, *11*, 3210-3215.

[5] Gross, R. A.; Kalra, B. Biodegradable Polymers for the Environment. *Science* **2002**, *297*, 803-807.

[6] Doppalapudi, S.; Jain, A.; Khan, W.; Domb, A. J. Biodegradable Polymers—an Overview. *Polym. Adv. Technol.* **2014**, *25*, 427-435.

[7] Gupta, A. P.; Kumar, V. New Emerging Trends in Synthetic Biodegradable Polymers – Polylactide: A Critique. *Eur. Polym. J.* **2007**, *43*, 4053-4074.

[8] Balasanthiran, V.; Chisholm, M. H.; Durr, C. B.; Gallucci, J. C. Single-Site Bismuth Alkoxide Catalysts for the Ring-Opening Polymerization of Lactide. *Dalton Trans.* **2013**, *42*, 11234-11241.

[9] Katsuki, T. Unique Asymmetric Catalysis of Cis -β Metal Complexes of Salen and Its Related Schiff-Base Ligands. *Chem. Soc. Rev.* **2004**, *33*, 437-444.

[10] Wang, X.; Liao, K.; Quan, D.; Wu, Q. Bulk Ring-Opening Polymerization of Lactides Initiated by Ferric Alkoxides. *Macromolecules* **2005**, *38*, 4611-4617.

[11] Shaver, M. P.; Cameron, D. J. A. Tacticity Control in the Synthesis of Poly(Lactic Acid) Polymer Stars with Dipentaerythritol Cores. *Biomacromolecules* **2010**, *11*, 3673-3679.

[12] Inkinen, S.; Hakkarainen, M.; Albertsson, A.-C.; Södergård, A. From Lactic Acid to Poly(Lactic Acid) (PLA): Characterization and Analysis of PLA and Its Precursors. *Biomacromolecules* **2011**, *12*, 523-532.

[13] Normand, M.; Dorcet, V.; Kirillov, E.; Carpentier, J. F. (Phenoxy-imine) Aluminum Versus-Indium Complexes for the Immortal ROP of Lactide: Different Stereocontrol, Different Mechanisms. *Organometallics* **2013**, *6*, 1694-1709.

[14] Dechy-Cabaret, O.; Martin-Vaca, B.; Bourissou, D. Controlled Ring-Opening Polymerization of Lactide and Glycolide. *Chem. Rev.* **2004**, *104*, 6147-6176.

[15] Ollevier, T. New Trends in Bismuth-catalyzed Synthetic Transformations. *Org. Biomol. Chem.* **2013**, *11*, 2740-2755.

[16] Bothwell, J. M.; Krabbe, S. W.; Mohan, R. S. Applications of Bismuth(III) Compounds in Organic Synthesis. *Chem. Soc. Rev.* **2011**, *40*, 4649-4707.

[17] Balasanthiran, V.; Chisholm, M. H.; Durr, C. B. Bismuth–lithium Bonding in the Ion Pairs: LiBiL2, Where L = a Porphyrin or a Salen Ligand. *Dalton Trans.* **2015**, *44*, 8205-8213.

[18] Loh, T. P.; Chua, G. L. Discovery of Indium Complexes as Water-tolerant Lewis Acids. *Chem. Comm.* **2006**, *26*, 2739-2749.

[19] Osten, K. M.; Mehrkhodavandi, P. Indium Catalysts for Ring Opening Polymerization: Exploring the Importance of Catalyst Aggregation. *Acc. Chem. Res.* **2017** *11*, 2861-2869.

[20] John, A.; Katiyar, V.; Pang, K.; Shaikh, M. M.; Nanavati, H.; Ghosh, P. Ni (II) and Cu (II) Complexes of Phenoxy-ketimine Ligands: Synthesis, Structures and Their Utility in Bulk Ring-Opening Polymerization (ROP) of L-lactide. *Polyhedron* **2007**, *15*, 4033-4044.

[21] Wei, Y.; Wang, S.; Zhou, S. Aluminum Alkyl Complexes: Synthesis, Structure, and Application in ROP of Cyclic Esters. *Dalton Trans.* **2016**, *11*, 4471-4485.

[22] Alesso, G.; Sanz, M.; Mosquera, M. E.; Cuenca, T. Monocyclopentadienyl Phenoxido–Amino and Phenoxido–Amido Titanium Complexes: Synthesis, Characterisation, and Reactivity of Asymmetric Metal Centre Derivatives. *Euro. J. Inorg. Chem.* **2008**, *29*, 4638-4649.

[23] Ma, M.; Shen, X.; Wang, W.; Li, J.; Yao, W.; Zhu, L. Syntheses of Sterically Bulky Schiff-Base Magnesium Complexes and Their Application in the Hydrosilylation of Ketones. *Eur. J. Inorg. Chem.* **2016**, *31*, 5057-5062.

[24] Benjamin, S. L.; Levason, W.; Reid, G.; Rogers, M. C.; Warr, R. P. Lewis Base Complexes of Methyldihalobismuthines $BiMeX_2$ (X= Cl or Br). *J. Organomet. Chem.* **2012**, *708*, 106-111.

[25] Bruker, *APEX2, SAINT, and SADABS. Bruker AXS Inc. Madison Wisconsin, USA.*, **2008.**

[26] Bruker, *APEX3, SAINT, and SADABS Bruker AXS Inc., Madison, Wisconsin, USA*, **2016.**

[27] G. M. Sheldrick, *Acta Crystallogr. A* **2015**, *71*, 3-8 (DOI:10.1107/S2053273314026370).

[28] G. M. Sheldrick, *Acta Crystallogr. C* **2015**, *71*, 3-8 (DOI:10.1107/S2053229614024218).

[29] Hubschle, C. B.; Sheldrick, G. M.; Dittrich, B. *J. Appl. Crystallogr.* **2011**, *44*, 1281-1284.

[30] Dolomanov, O. V.; Bourhis, L. J.; Gildea, R. J.; Howard J. A. K.; Puschmann, H. *J. Appl. Crystallogr.* **2009**, *42*, 339-341.

[31] Cameron, P. A.; Gibson, V. C.; Redshaw, C.; Segal, J. A.; Solan, G. A.; White, A. J.; Williams, D. J. Synthesis and Characterisation of Neutral Dialkylaluminium Complexes Stabilised by Salicylaldiminato Ligands, and their Conversion to Monoalkylaluminium Cations. *Dalton Trans.* **2001**, *9*, 1472-1476.

7. Appendix

Appendix 1. ^{1}H NMR spectrum of **HL1**.

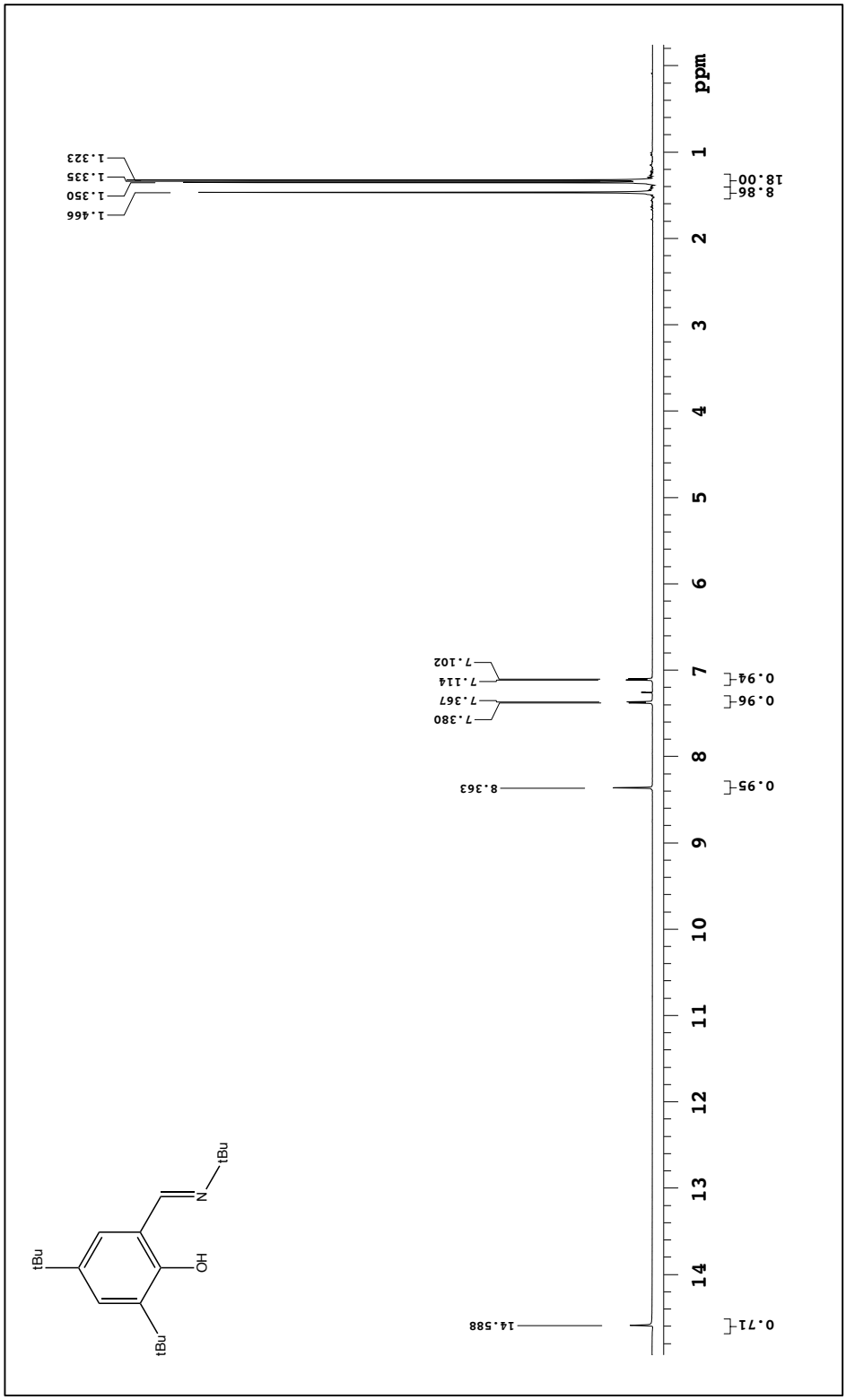

Appendix 2. ^{1}H NMR spectrum of **HL2**.

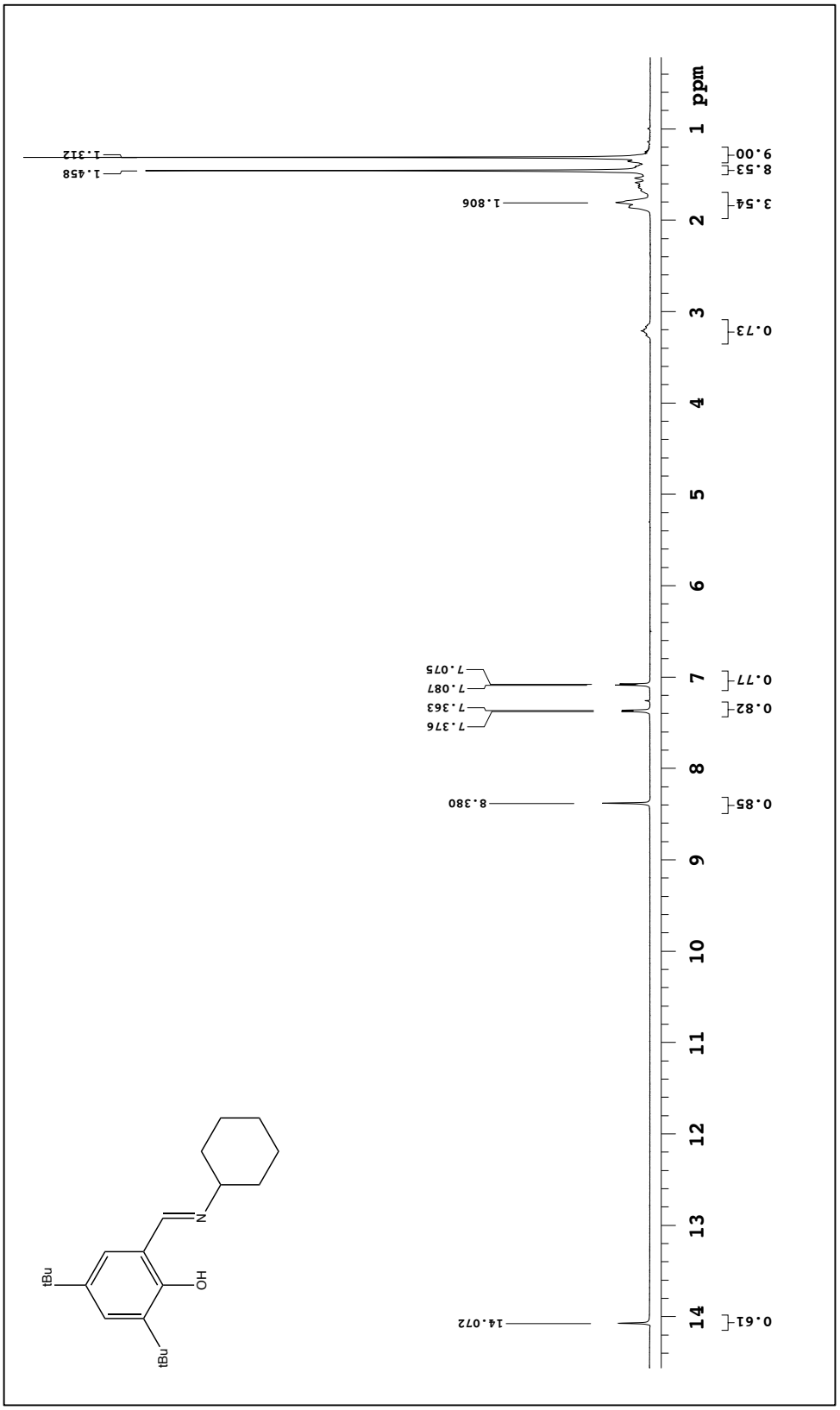

Appendix 3. ^{1}H NMR spectrum of **HL3**.

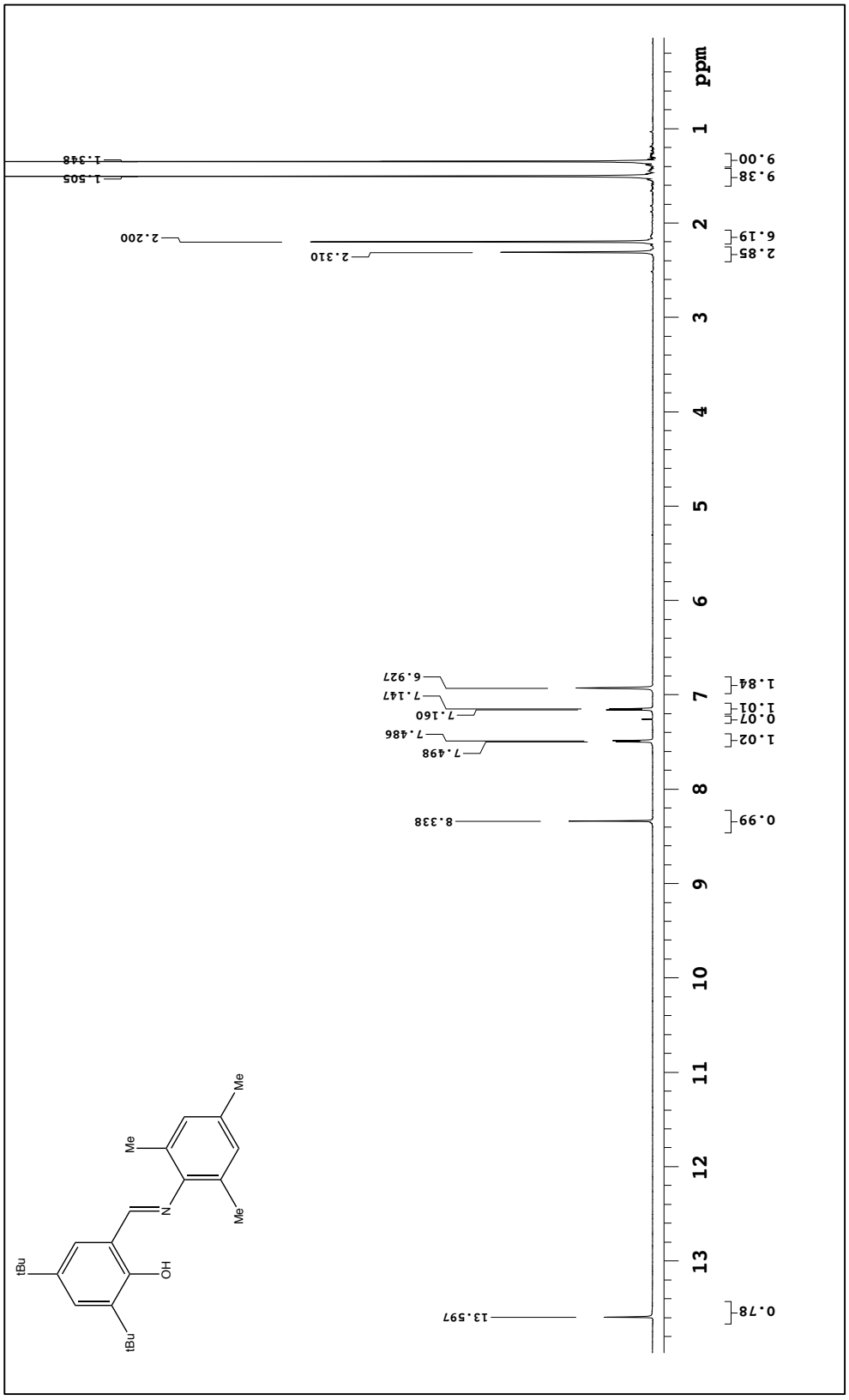

Appendix 4. ^{1}H NMR spectrum of **NaL1**.

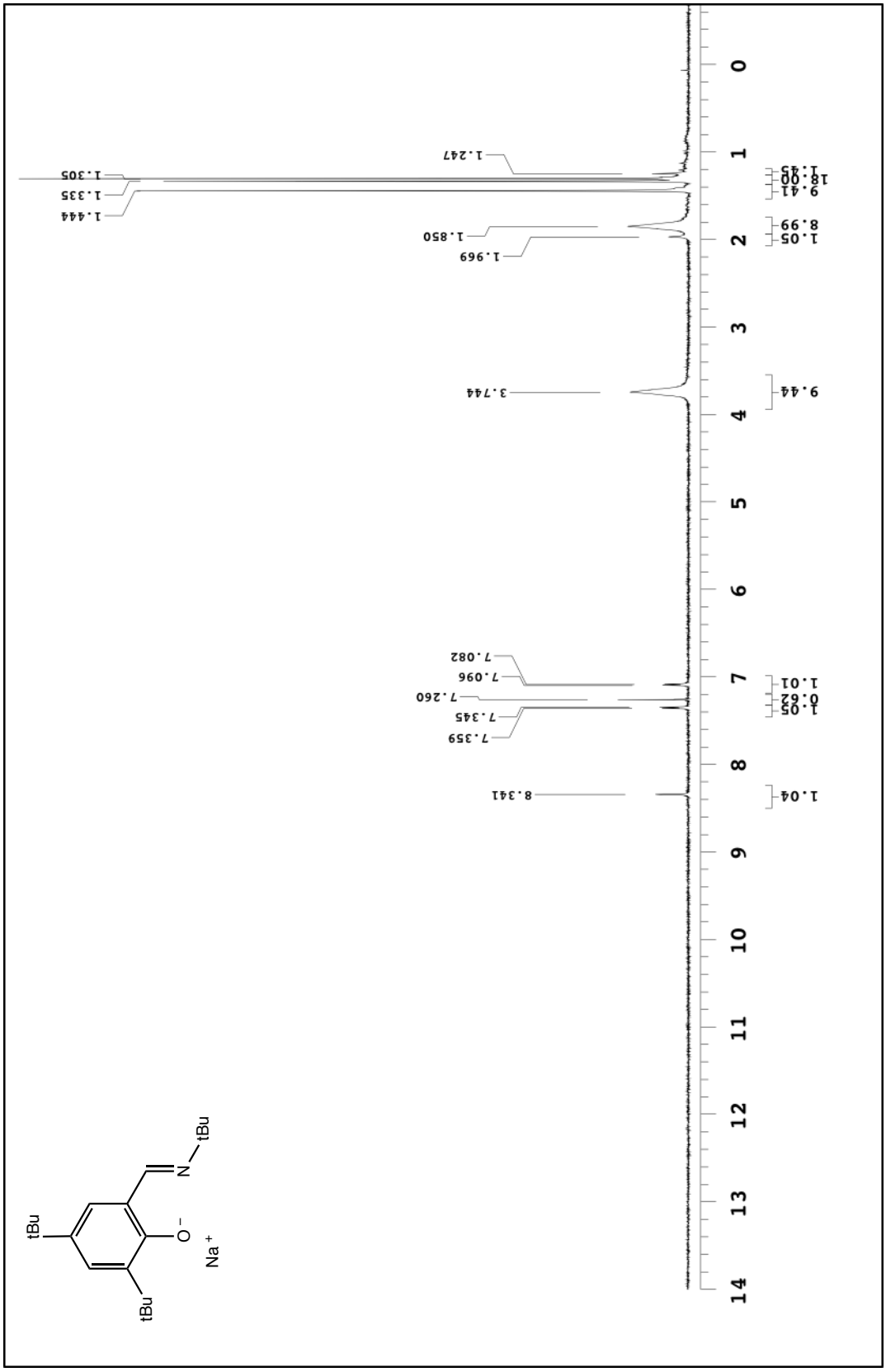

Appendix 5. ^{1}H NMR spectrum of **NaL2**.

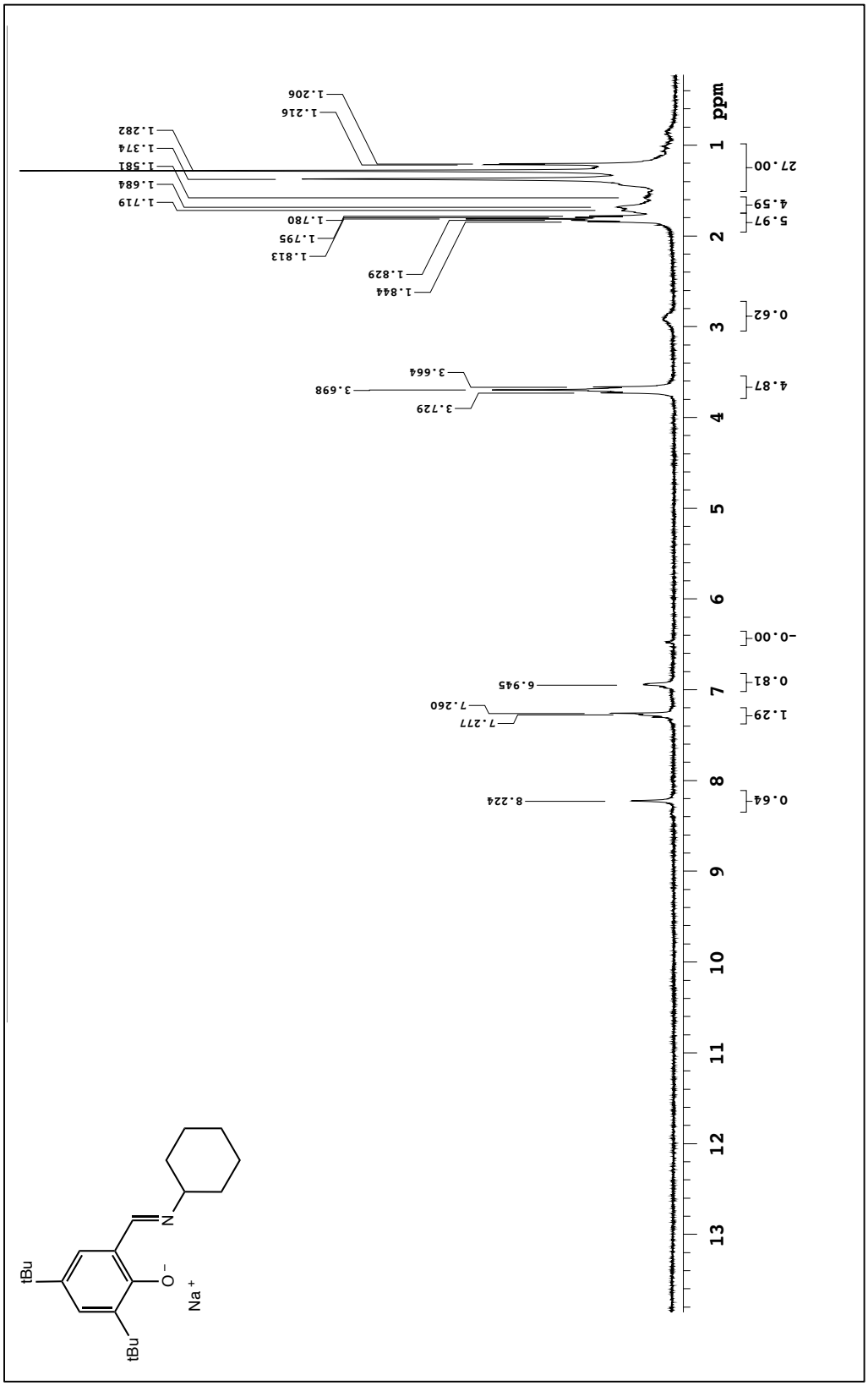

Appendix 6. ^{1}H NMR spectrum of **NaL3**.

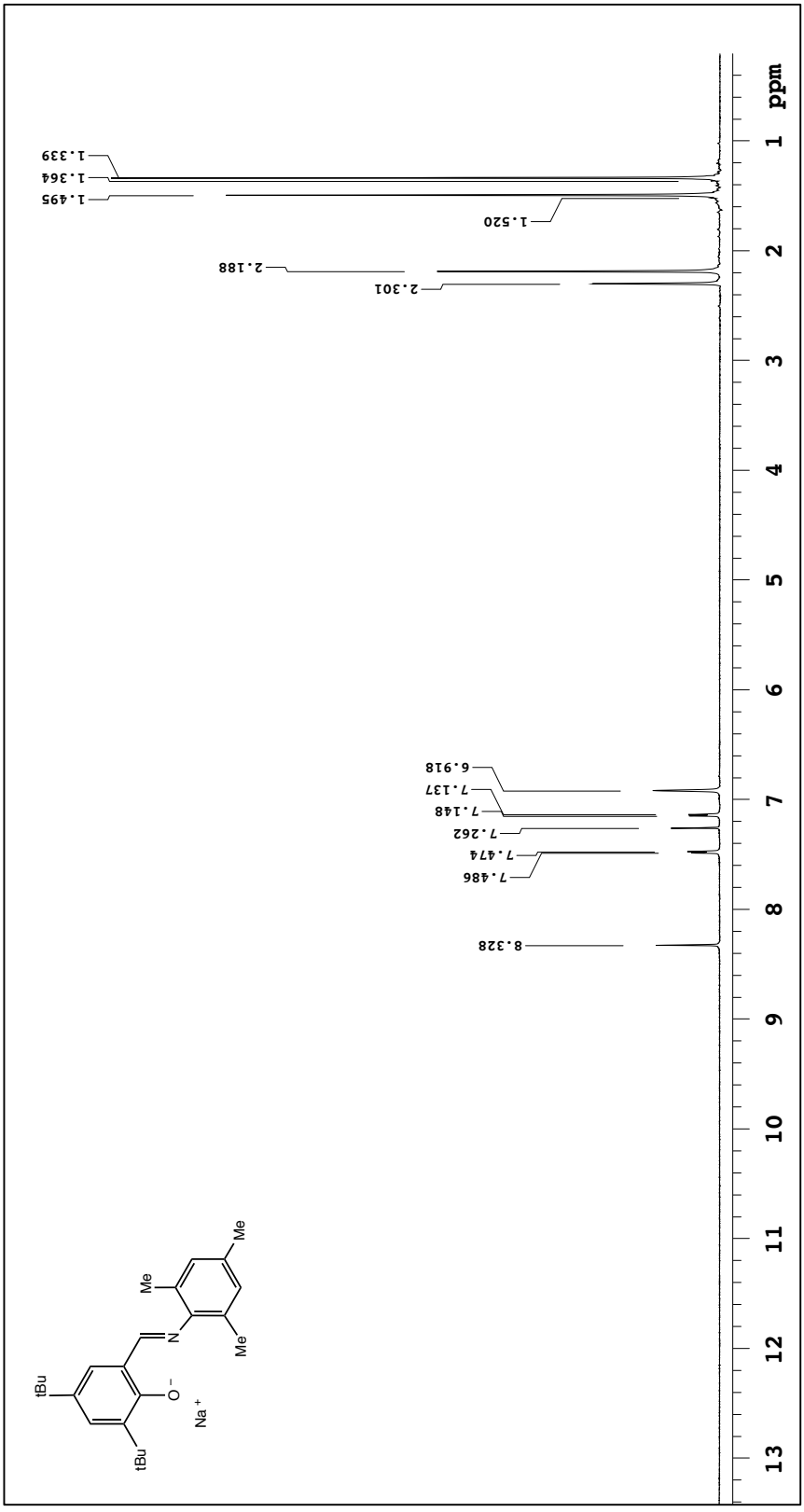

Appendix 7. ^{1}H NMR spectrum of **Me_2BiBr**.

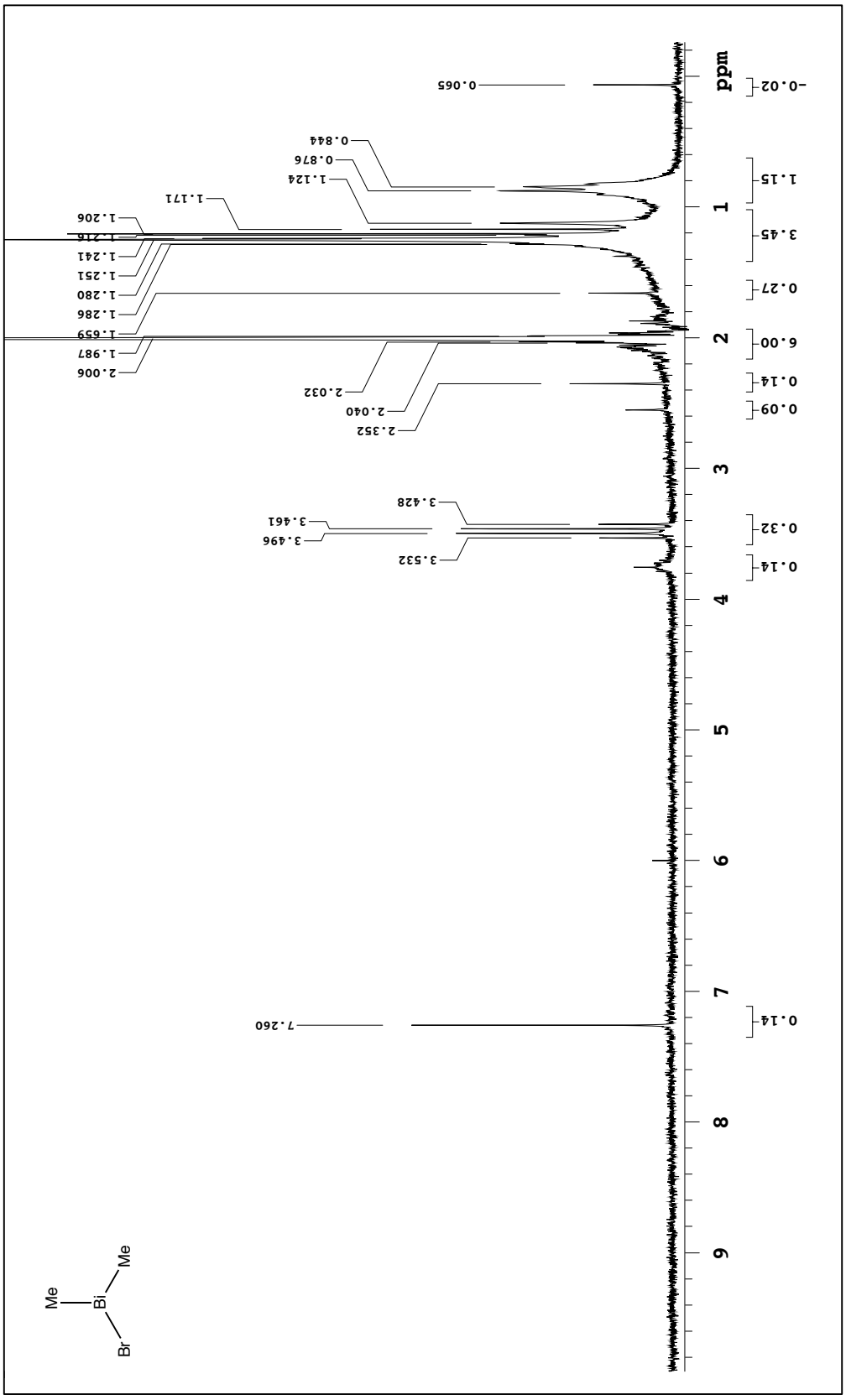

Appendix 8. ^{1}H NMR spectrum of **1**.

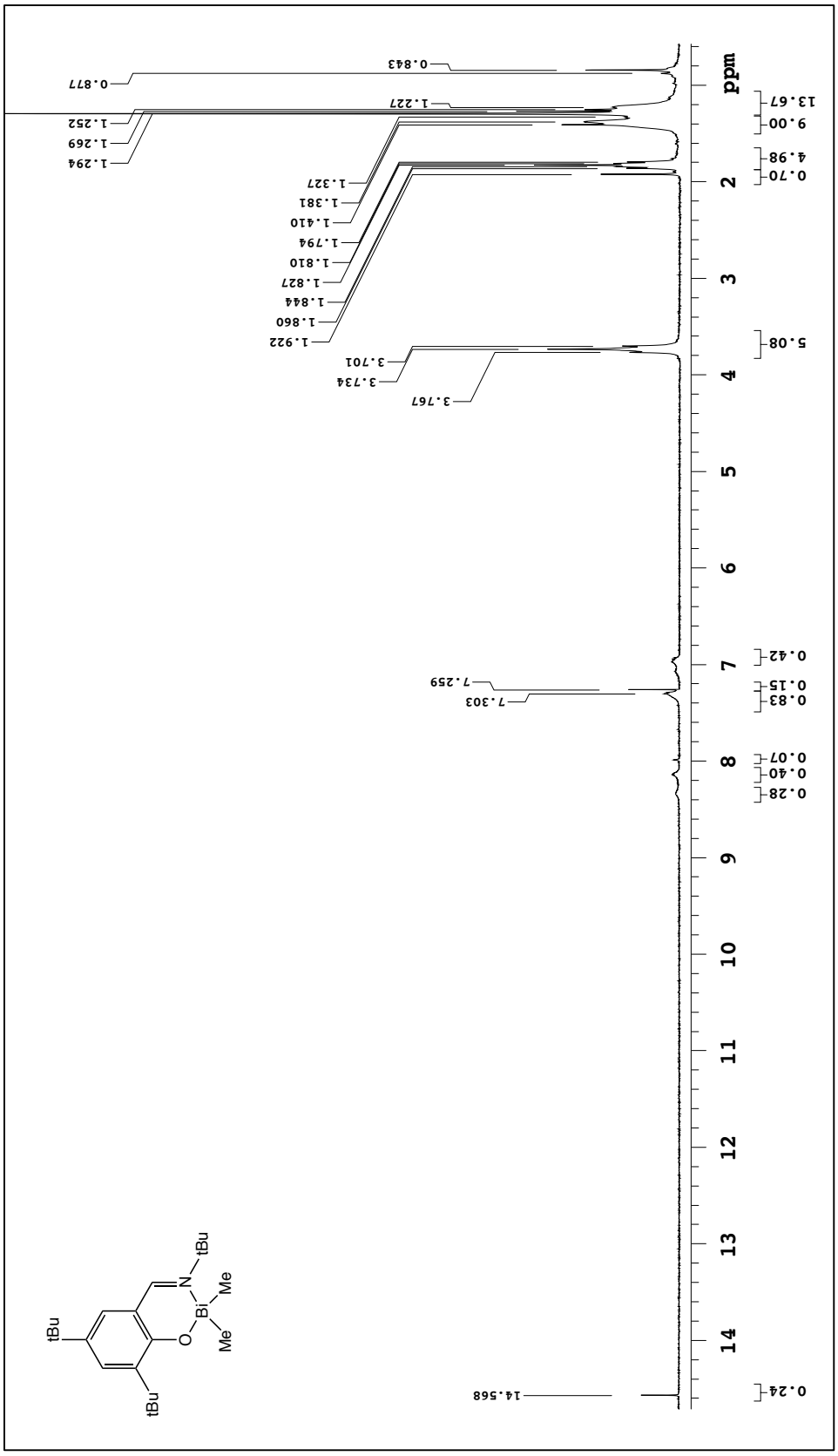

Appendix 9. ^{1}H NMR spectrum of **2**.

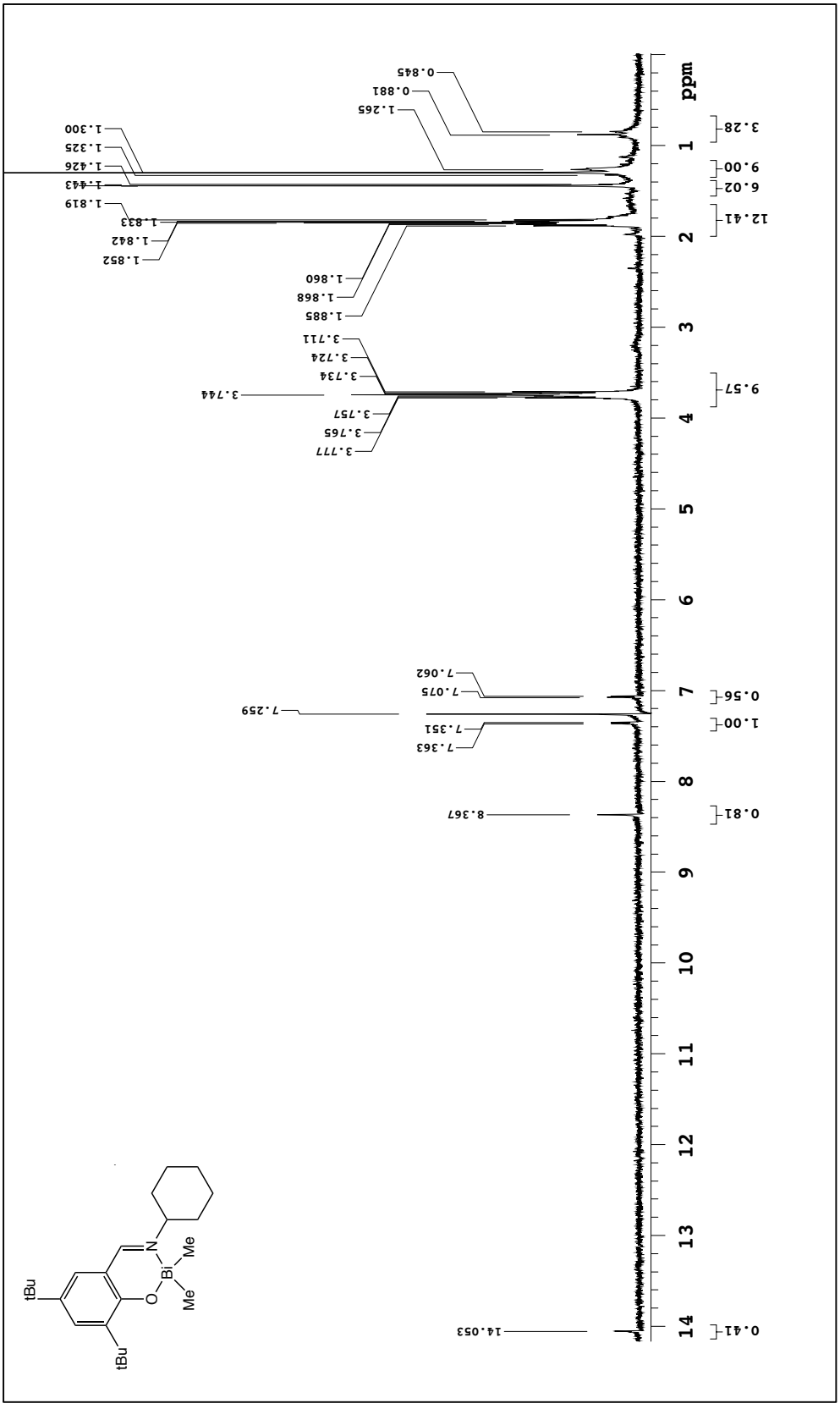

Appendix 10. ^{1}H NMR spectrum of **3**.

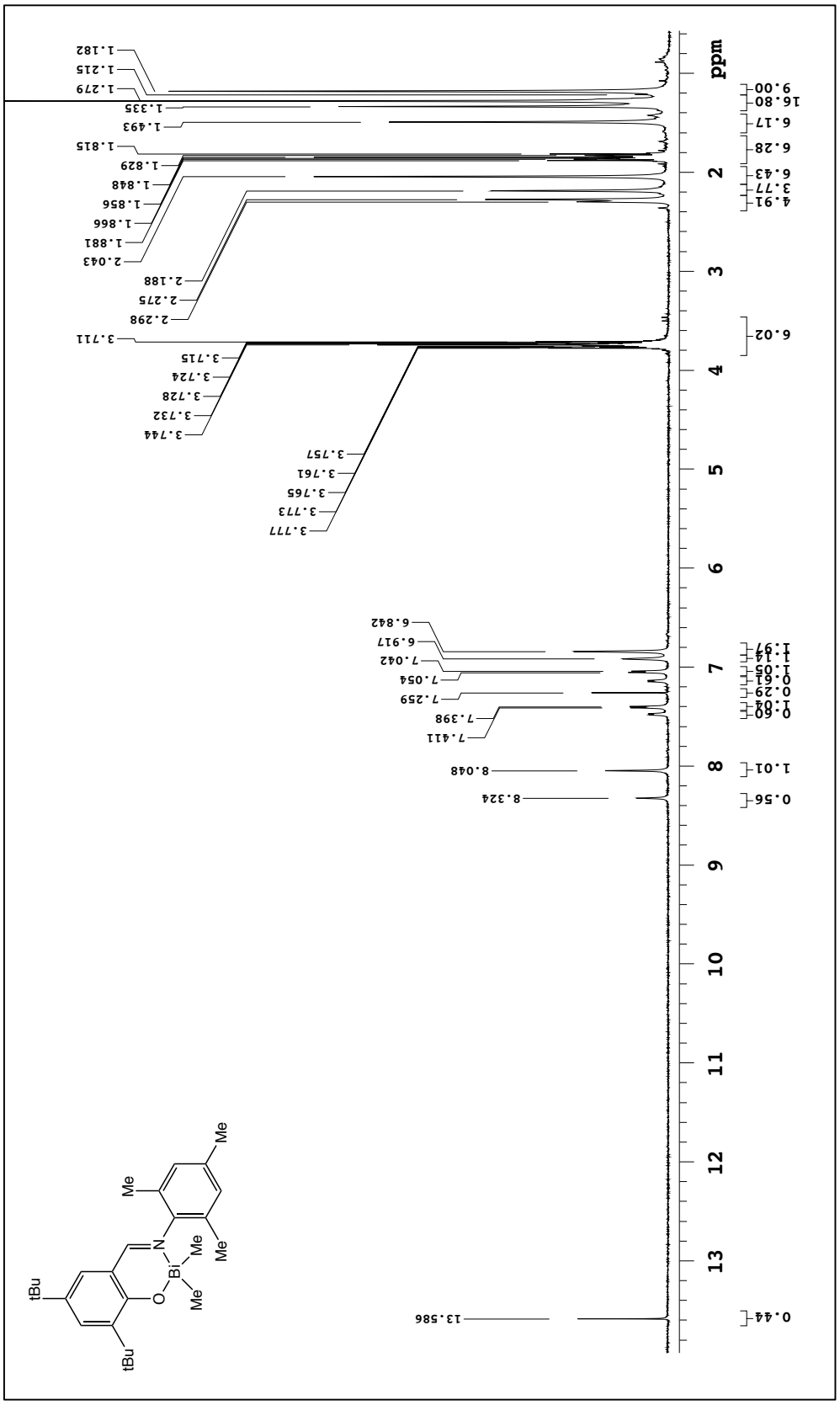

Appendix 11. FT-Raman spectrum of **3**.

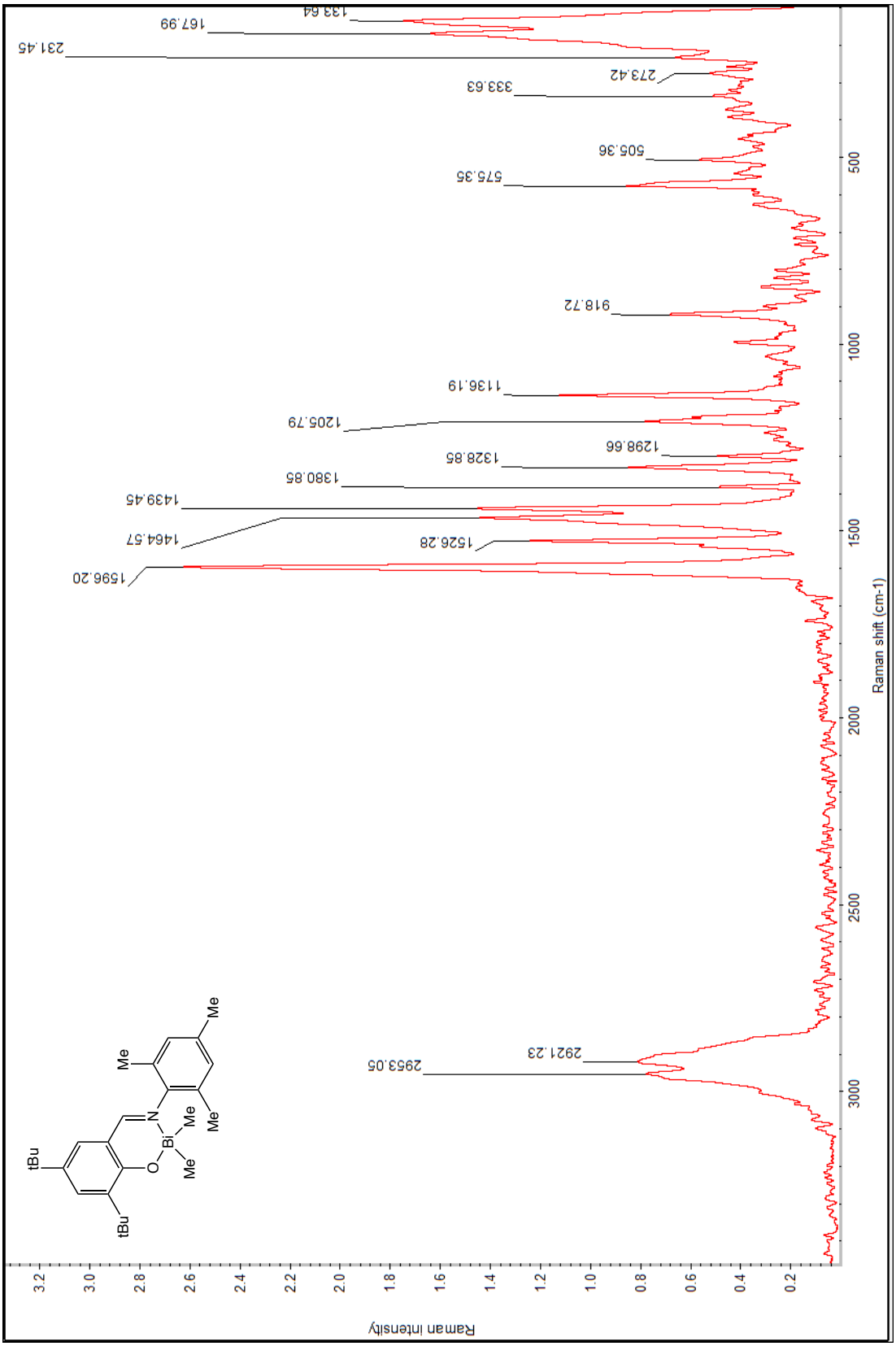

Appendix 12. ^{1}H NMR spectrum of **4.**

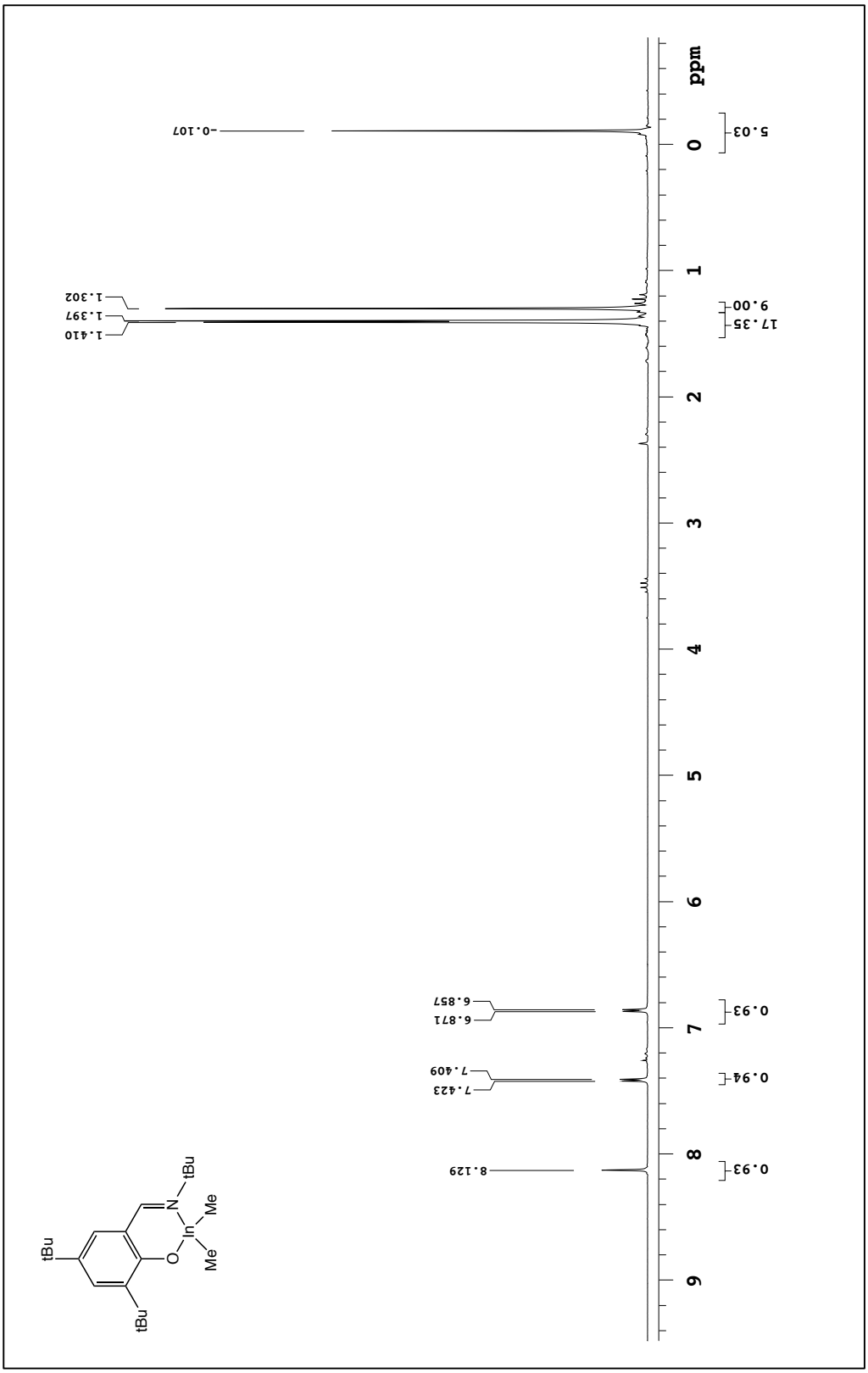

Appendix 13. $^{13}C\{^{1}H\}$ NMR spectrum of **4**.

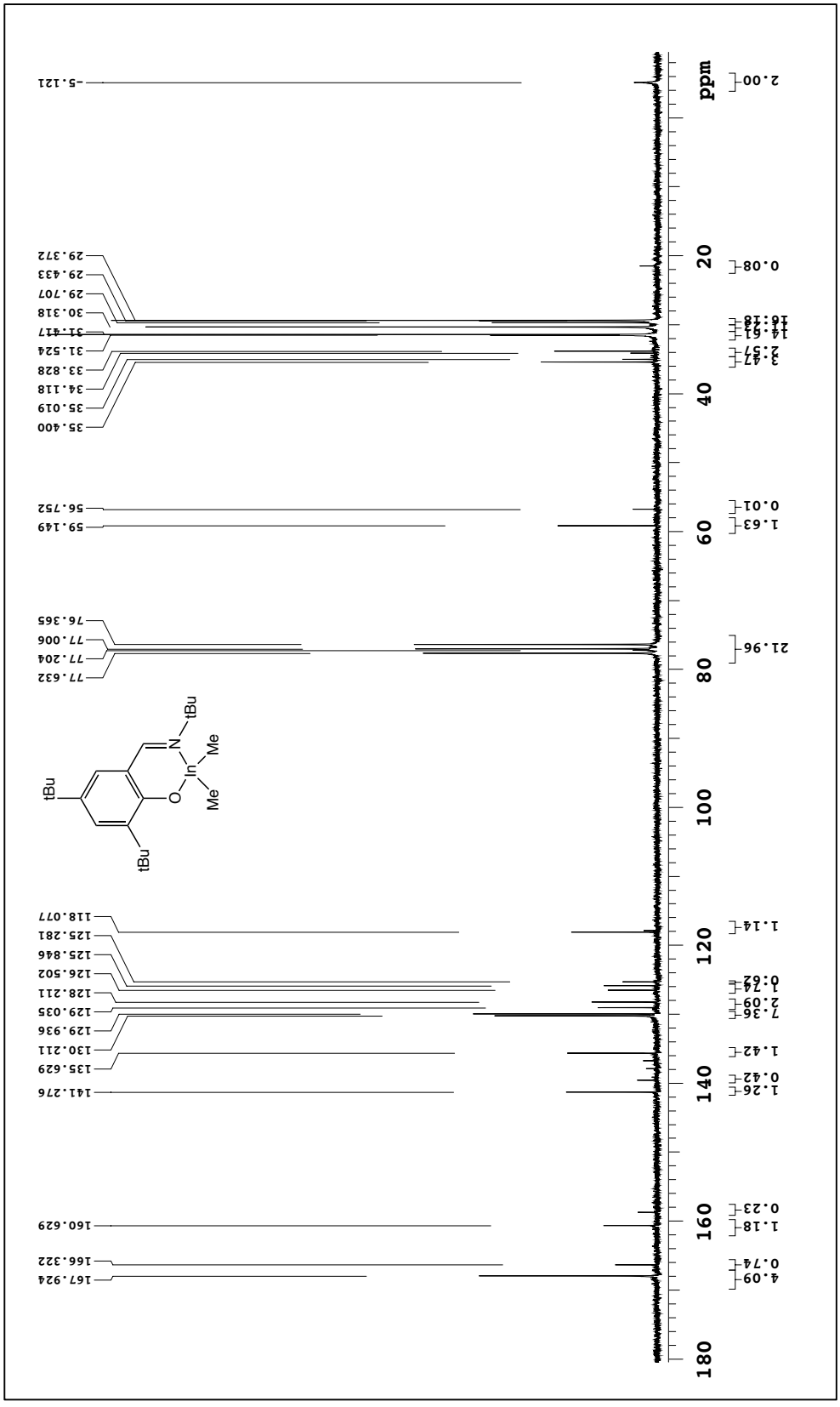

Appendix 14. FT-Raman spectrum of **4**.

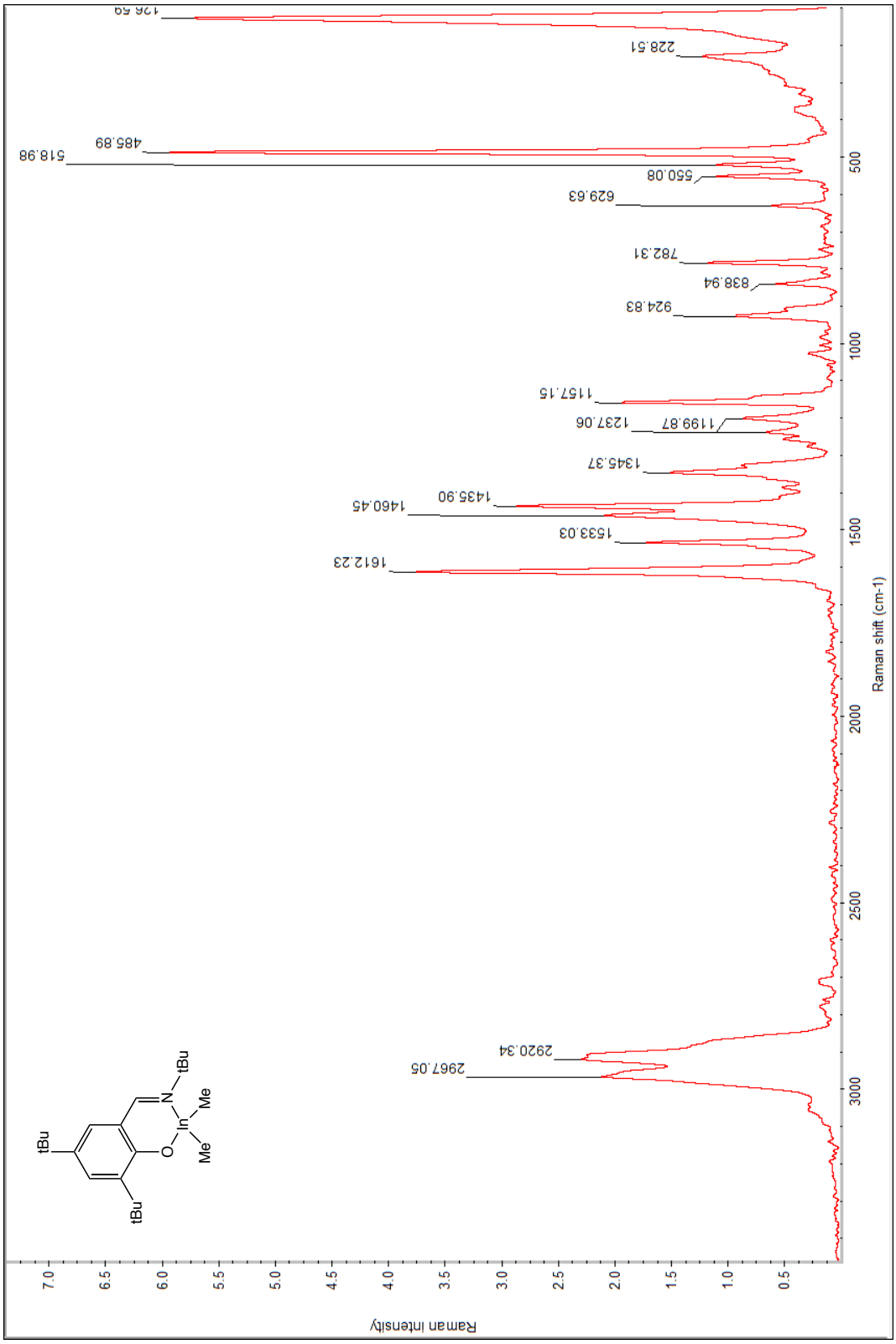

Appendix 15. FT-IR spectrum of **4**.

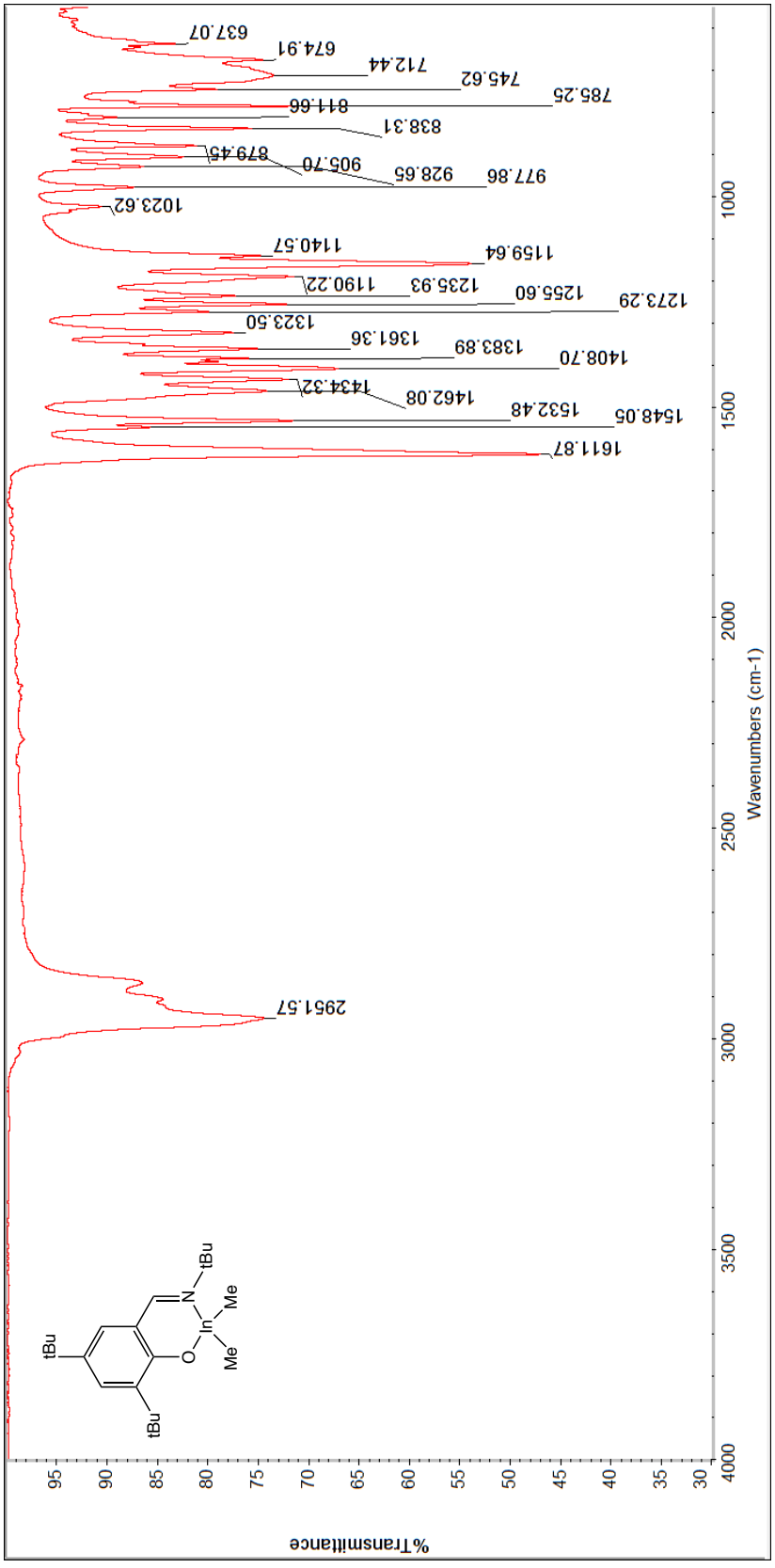

Appendix 16. ^{1}H NMR spectrum of **5**.

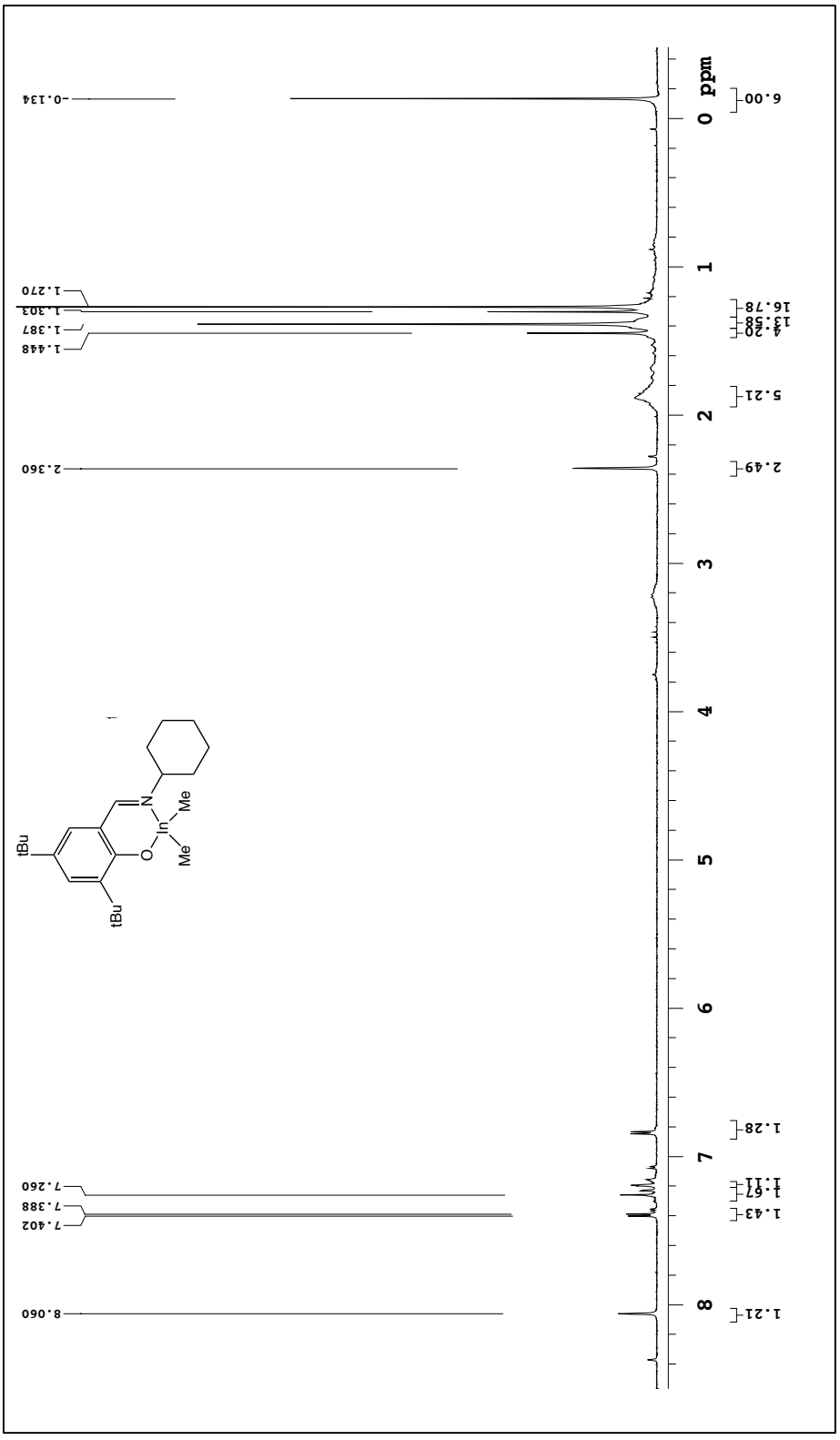

Appendix 17. $^{13}C\{^{1}H\}$ NMR spectrum of **5**.

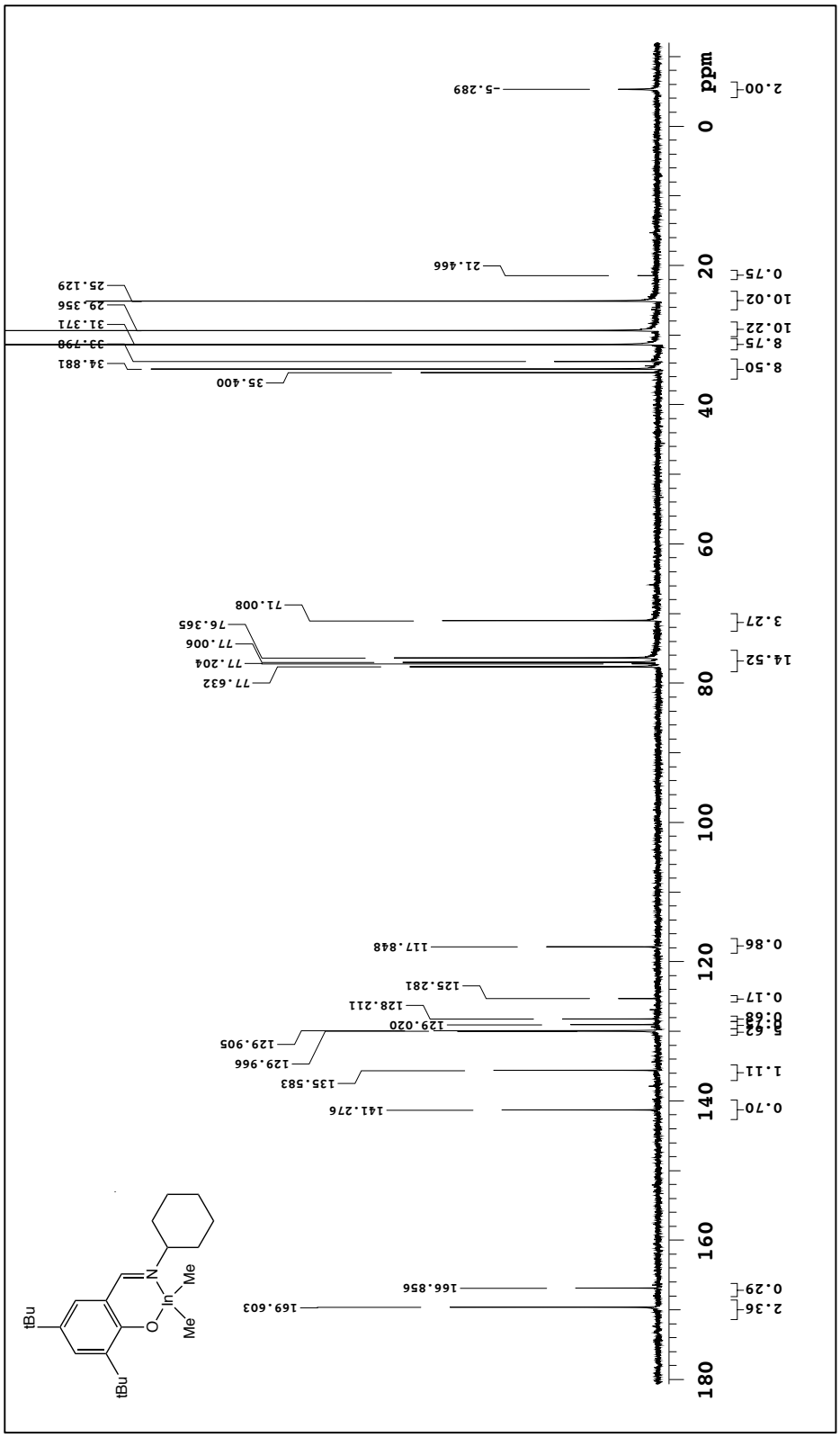

Appendix 18. FT-Raman spectrum of **5**.

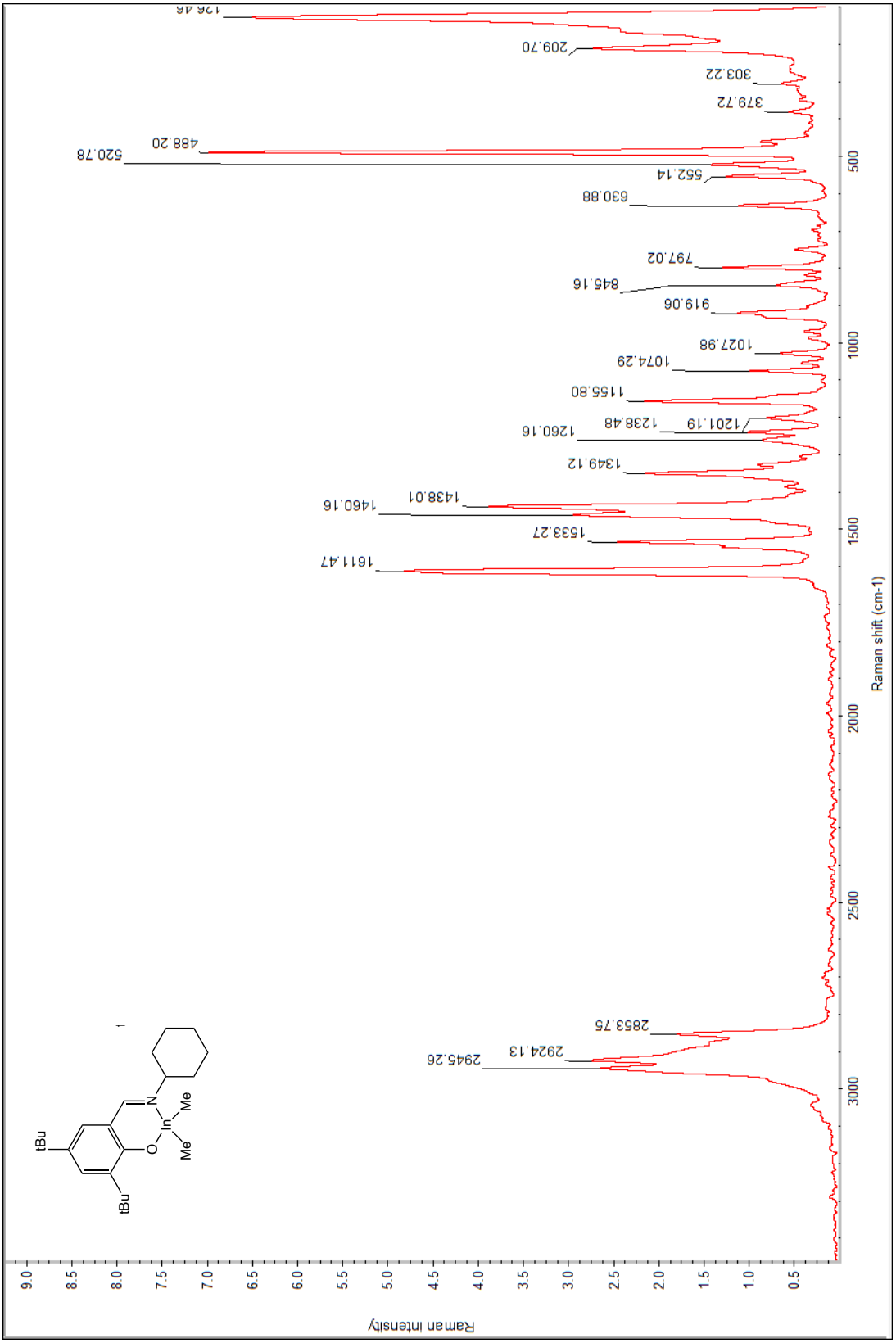

Appendix 18. FT-IR spectrum of **5**.

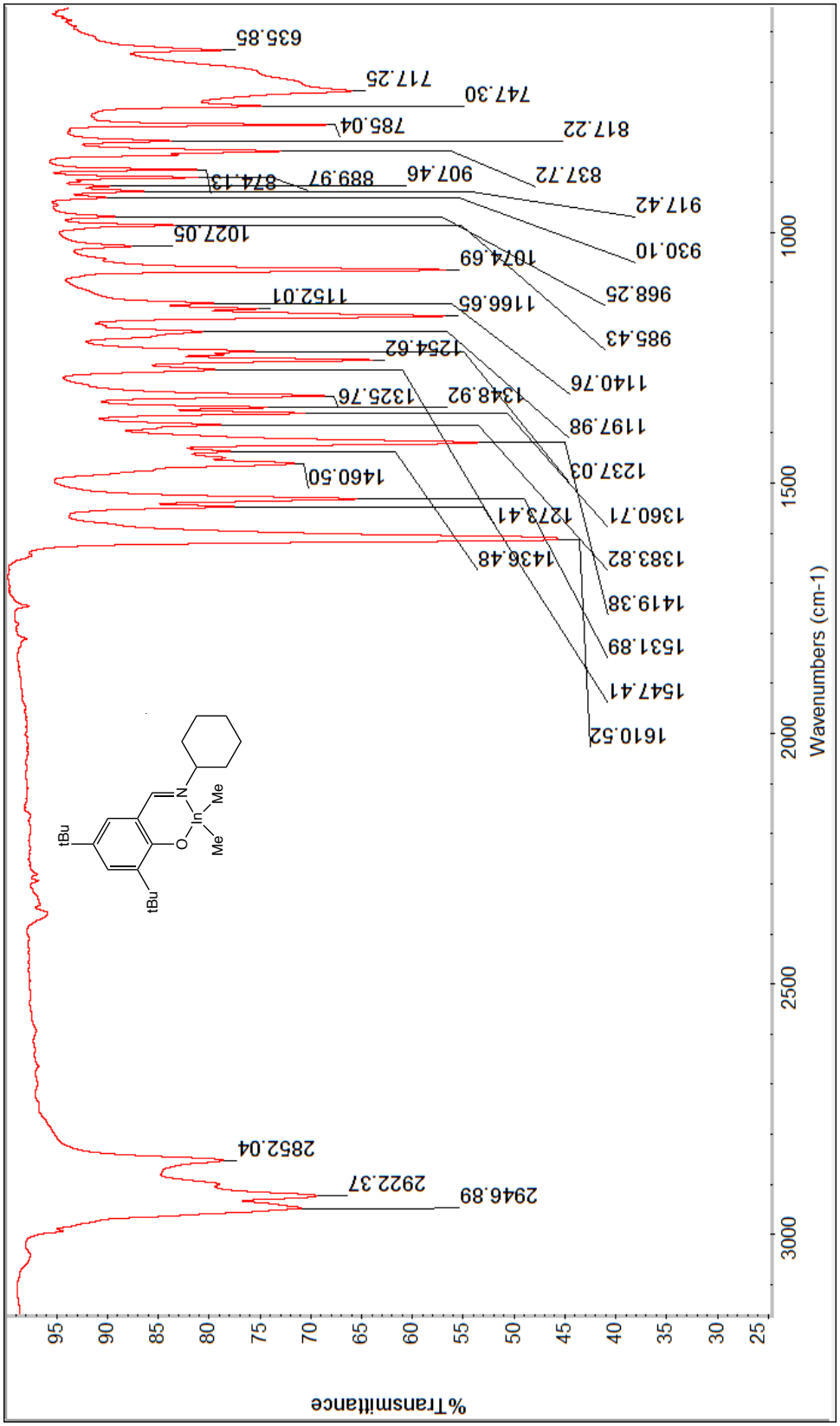

Appendix 20. ^{1}H NMR spectrum of **6**.

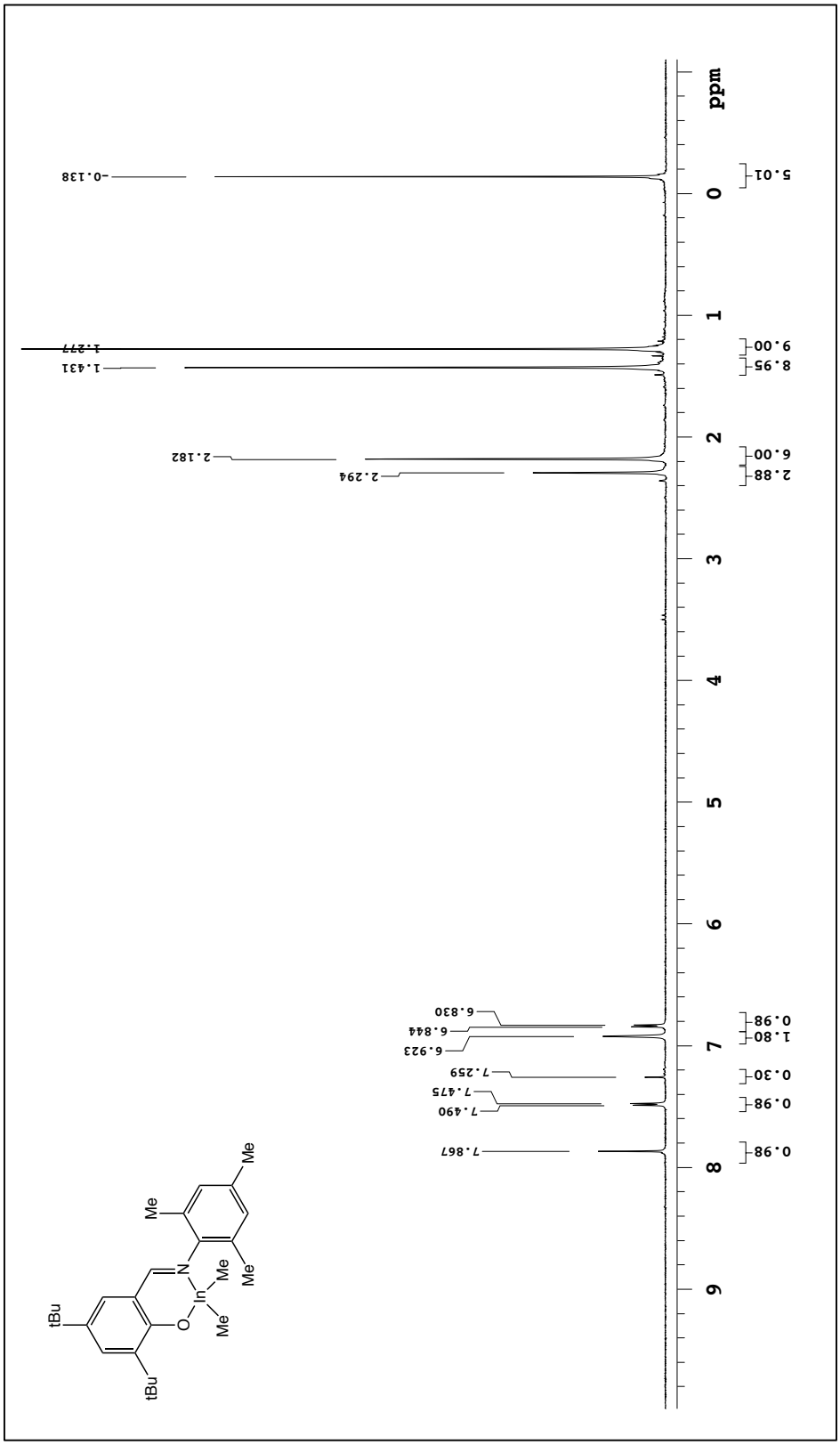

Appendix 21. $^{13}C\{^{1}H\}$ NMR spectrum of **6**.

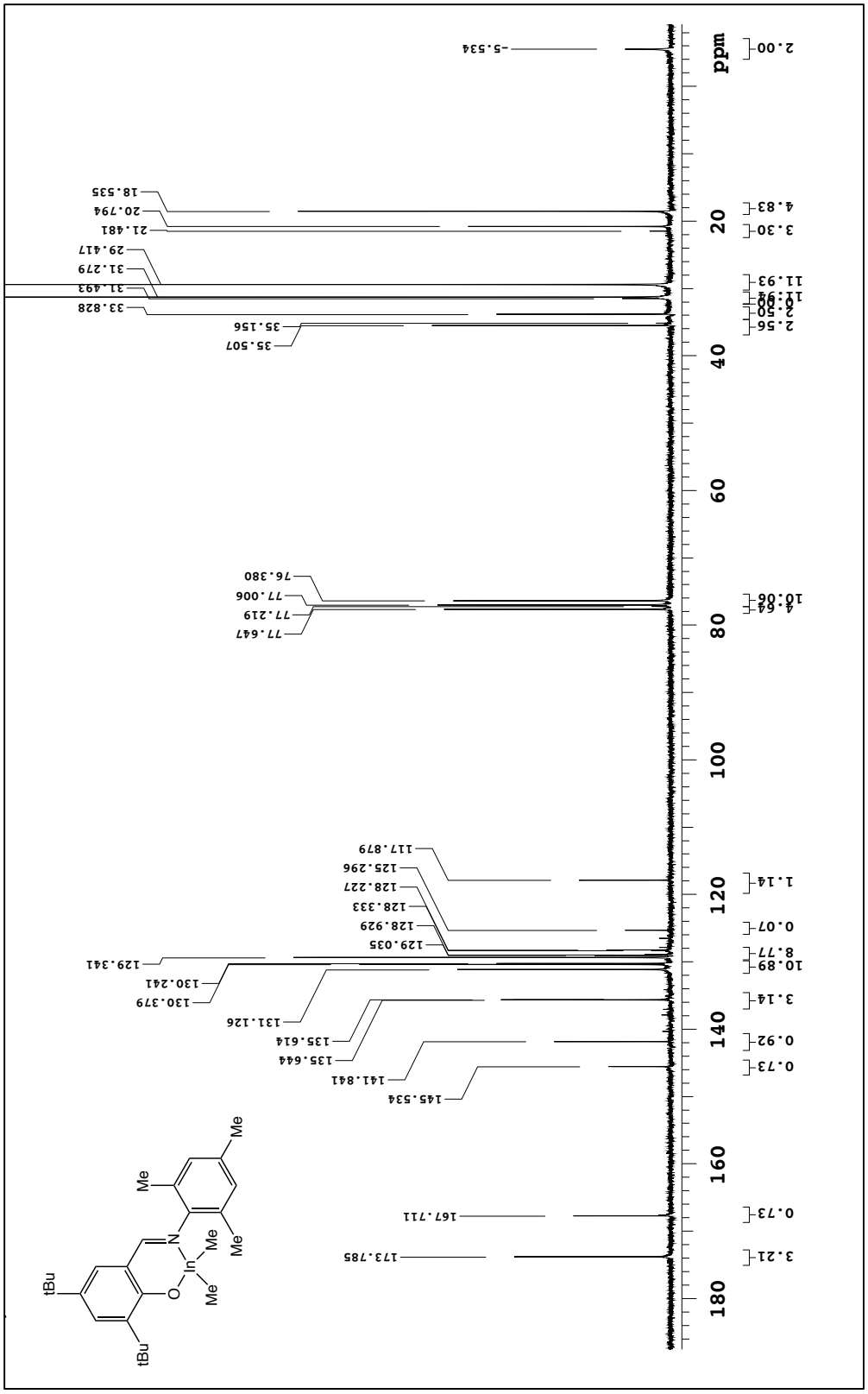

Appendix 22. FT-Raman spectrum of **6**.

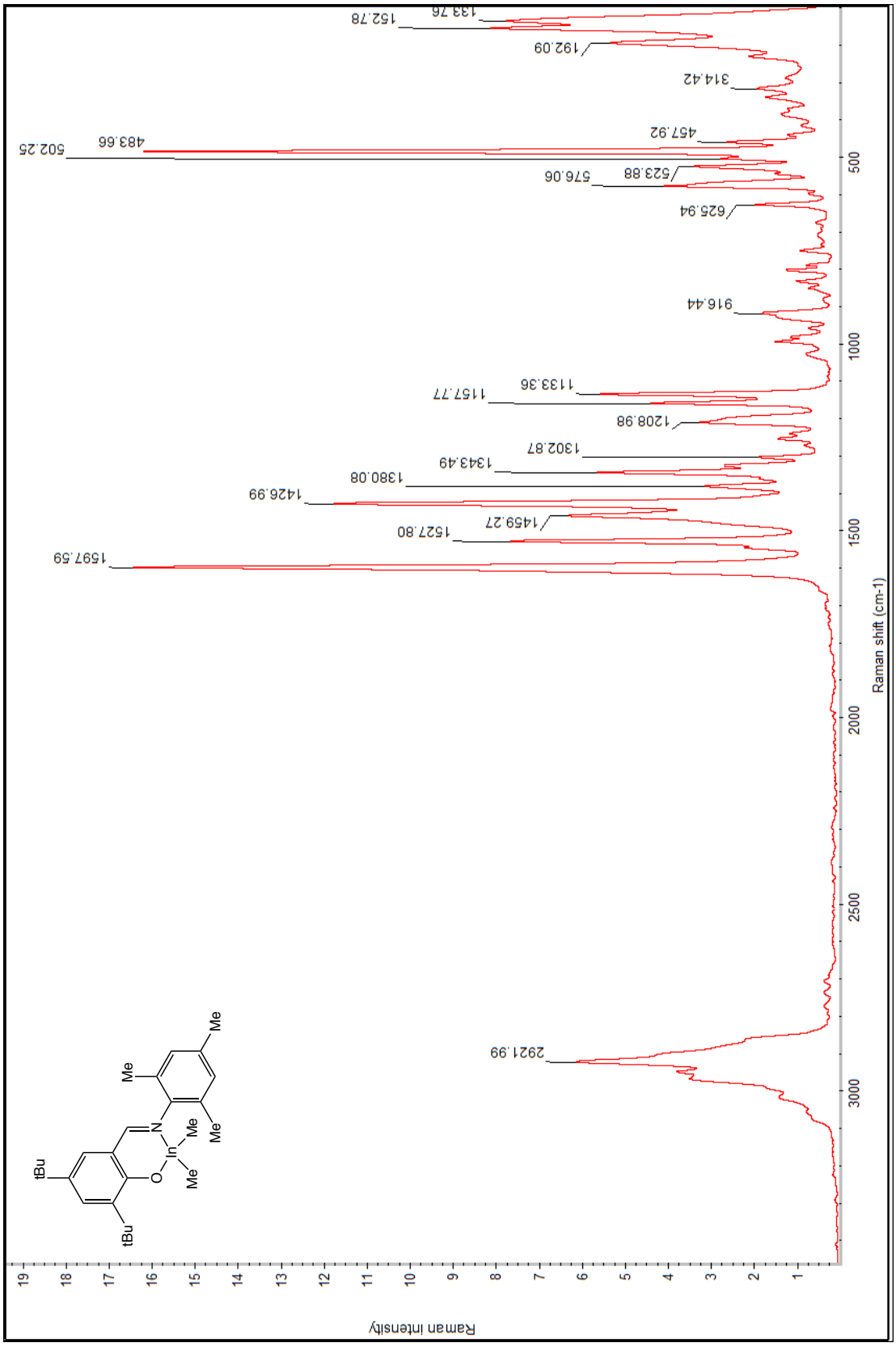

Appendix 23. FT-IR spectrum of **6**.